



**HAL**  
open science

# Lacustrine rhythmites from the Mulhouse Basin (Upper Rhine Graben, France): a sedimentary record of increased seasonal climatic contrast and sensitivity of the climate to orbital variations through the Eocene-Oligocene Transition

Emile Simon, Laurent Gindre-Chanu, Cécile Blanchet, Guillaume Dupont-Nivet, Mathieu Martinez, François Guillocheau, Marc Ulrich, Alexis Nutz, Hendrik Vogel, Mathieu Schuster

## ► To cite this version:

Emile Simon, Laurent Gindre-Chanu, Cécile Blanchet, Guillaume Dupont-Nivet, Mathieu Martinez, et al.. Lacustrine rhythmites from the Mulhouse Basin (Upper Rhine Graben, France): a sedimentary record of increased seasonal climatic contrast and sensitivity of the climate to orbital variations through the Eocene-Oligocene Transition. *Sedimentologica*, 2024, 2 (1), 10.57035/journals/sdk.2024.e21.1222 . insu-04485737v2

**HAL Id: insu-04485737**

**<https://insu.hal.science/insu-04485737v2>**

Submitted on 25 Mar 2024

**HAL** is a multi-disciplinary open access archive for the deposit and dissemination of scientific research documents, whether they are published or not. The documents may come from teaching and research institutions in France or abroad, or from public or private research centers.


L'archive ouverte pluridisciplinaire **HAL**, est destinée au dépôt et à la diffusion de documents scientifiques de niveau recherche, publiés ou non, émanant des établissements d'enseignement et de recherche français ou étrangers, des laboratoires publics ou privés.



Distributed under a Creative Commons Attribution 4.0 International License



# Lacustrine rhythmites from the Mulhouse Basin (Upper Rhine Graben, France): a sedimentary record of increased seasonal climatic contrast and sensitivity of the climate to orbital variations through the Eocene-Oligocene Transition

Emile Simon<sup>1\*</sup> , Laurent Gindre-Chanu<sup>2</sup>, Cécile Blanchet<sup>3</sup> , Guillaume Dupont-Nivet<sup>3,4</sup> , Mathieu Martinez<sup>4</sup> , François Guillocheau<sup>4</sup>, Marc Ulrich<sup>1</sup> , Alexis Nutz<sup>5</sup>, Hendrik Vogel<sup>6</sup> , Mathieu Schuster<sup>1\*</sup> 

- <sup>1</sup> Université de Strasbourg, CNRS, Institut Terre et Environnement de Strasbourg, UMR 7063, 5 rue Descartes, Strasbourg F-67084, France  
<sup>2</sup> TERRA GEOSCIENCES, 3 Bis rue des Marmuzots, 21000 Dijon, France  
<sup>3</sup> Helmholtz Centre Potsdam GFZ, German Research Centre for Geosciences, Telegrafenberg, 14473 Potsdam, Germany  
<sup>4</sup> Géosciences Rennes, UMR CNRS 6118, Rennes, 35042 Rennes Cedex, France  
<sup>5</sup> CEREGE, Aix-Marseille Université, CNRS, IRD, Collège de France, INRAE, Aix en Provence, France  
<sup>6</sup> Institute of Geological Sciences & Oeschger Centre for Climate Change Research, University of Bern, Baltzerstrasse 1+3, 3012 Bern, Switzerland

\*corresponding authors: Emile Simon ([emile.simon.geology@gmail.com](mailto:emile.simon.geology@gmail.com))  
Mathieu Schuster ([mschuster@unistra.fr](mailto:mschuster@unistra.fr))

doi: [10.57035/journals/sdk.2024.e21.1222](https://doi.org/10.57035/journals/sdk.2024.e21.1222)

Editors: Suzanne Bull, and Katrina Kremer  
Reviewers: Nicolas Waldmann and Ola Kwiecien  
Copyediting, layout and production: Romain Vaucher, Thomas J.H. Dodd and Liz Mahon

Submitted: 30.06.2023  
Accepted: 29.01.2024  
Published: 26.02.2024

**Abstract** | The Eocene-Oligocene Transition (EOT) marks the passage from Eocene greenhouse to Oligocene icehouse conditions. It holds keys to our understanding of the behavior of climate systems under major pCO<sub>2</sub> shifts. While the environmental impact of the EOT is rather homogenous in oceans, it is much more heterogeneous on continents. Although little to no changes are recorded in some regions, several EOT studies in western Eurasia suggest an increase in seasonal climatic contrast (e.g., higher amplitude of changes in mean temperature or precipitation), along with a higher sensitivity of the climate to orbital variations. However, these variations remain to be properly documented through changes in sedimentary facies and structures and forcing mechanisms. Here we investigate the depocenter of the Mulhouse Basin (Upper Rhine Graben; URG) revealing a prominent transition from massive mudstones to laminated sediments and varves, alongside the emergence of astronomically-forced mudstone-evaporite alternations. These changes are identified in the distal and proximal parts of the southern URG, where they consist of millimeter-thick mudstone-evaporite couplets and siliciclastic-carbonate couplets. The elemental composition and micro-facies analysis of the laminae show a recurrent depositional pattern consistent with a seasonal depositional process, which suggests that they are varves. We propose that the occurrence of varved sediments, together with the observed orbital cyclicity in the southern URG, reflects an increase in seasonal climatic contrast, and an increase in the sensitivity of climate to orbital variations across the EOT. We show that similar changes were noticed in the Rennes and Bourg-en-Bresse basins, and that of other western Eurasian records for similar climatic conditions. This work emphasizes the potential of high-resolution sedimentary structures to serve as markers of climate change across the EOT.

**Résumé** | La Transition Éocène-Oligocène (TEO) marque le passage des conditions « greenhouse » de l'Éocène aux conditions « Icehouse » de l'Oligocène. Son étude nous permet de mieux comprendre les réponses des systèmes climatiques à des variations majeures de taux de pCO<sub>2</sub>. Tandis que l'impact environnemental de la TEO est plutôt homogène dans le domaine océanique, de fortes hétérogénéités sont observées sur les continents. Bien que certaines régions montrent peu de changements, plusieurs études de la TEO suggèrent une augmentation du contraste climatique saisonnier (e.g., plus grande amplitude des changements de la température moyenne et des précipitations), ainsi qu'une plus grande sensibilité du climat aux variations orbitales. Toutefois, ces variations n'étaient pas encore documentées à travers des changements de faciès, de structures sédimentaires, et des mécanismes de forçages. Nous avons étudié ici le dépocentre du bassin de Mulhouse (Fossé Rhénan) qui révèle une transition importante entre des

mudstones massives vers des sédiments laminés et des varves, ainsi que l'émergence d'alternances mudstone-évaPORITE décimétriques liées aux variations orbitales. Ces structures sont identifiées dans les parties distales et proximales du Fossé Rhénan méridional, où l'on observe des couplets mudstone-évaPORITE et des couplets clastique-carbonate millimétriques. La composition élémentaire et l'analyse des micro-faciès des lamines montrent un schéma de dépôt récurrent compatible avec un processus de dépôts saisonnier, ce qui suggère qu'il s'agit de varves. Nous proposons que l'émergence de varves et de cyclicité orbitale observée dans le Fossé Rhénan méridional reflètent une augmentation du contraste climatique saisonnier, et une augmentation de la sensibilité du climat aux variations orbitales à travers la TEO. Nous montrons que des changements similaires existent dans les bassins de Rennes et de Bourge-en-Bresse, et que d'autres enregistrements sédimentaires d'Eurasie témoignent de conditions climatiques semblables. Ce travail souligne le fort potentiel des structures sédimentaires de haute résolution comme marqueurs de changements climatique à travers la TEO.

**Lay summary |** The Eocene-Oligocene Transition (EOT) marks the shift from greenhouse to modern icehouse conditions. It is a crucial event to document in order to better understand climate change processes. We studied the lacustrine record of the Mulhouse Basin (Upper Rhine Graben, France) to document the impacts of the EOT on the continental environments of this rift basin. We highlight two major changes in sedimentary deposition patterns. The first is a transition from massive mudstones to finely laminated sediments and varves. The second is the concomitant onset of decameter-thick mudstone-évaPORITE cycles related to orbital variations. We interpret these changes as induced by an increase in seasonal climatic contrast and in the sensitivity of the climate to orbital variations across the EOT. We show that other continental basins in Eurasia recorded similar sedimentary changes at that time, suggesting a tight link between Eurasian climates and Antarctic icesheets. We highlight the potential of sedimentary structures as sedimentary markers of climate change at the EOT.

**Keywords:** Eocene-Oligocene Transition, Seasonality, Varves, Lake, Upper Rhine Graben

## 1. Introduction

The Eocene-Oligocene Transition (EOT) climatic event (~33.9 Ma) is marked by a strong oxygen isotopic shift globally recorded in oceanic benthic foraminifera, interpreted as a combination of a drop in temperature and development of the Antarctic ice-sheet (Zachos et al., 2001; Miller et al., 2020; Hutchinson et al., 2021). Data from deep marine carbon and oxygen stable isotope records suggest that the EOT occurred in several steps. Two major events are the EOT-1 and Oi-1, which are associated with cooling and formation of the Antarctic ice-sheet, respectively. The Oi-1 event resulted in a ca. 70 m eustatic sea-level drop (Miller et al., 1991; Zachos et al., 2001; Coxall et al., 2005; Katz et al., 2008; Kennedy et al., 2015; Hutchinson et al., 2021). Two main mechanisms underpinning the EOT have been proposed: (1) the decrease in atmospheric pCO<sub>2</sub>, which likely passed a threshold value (DeConto & Pollard, 2003; Pearson et al., 2009; Toumoulin et al., 2022), and/or (2) changes in oceanic gateways (e.g., Atlantic-Arctic, Southern Ocean, and Mesopotamian), which possibly initiated the Antarctic Circumpolar Current (ACC) (Kennett, 1977; Sarkar et al., 2019). Initiation and/or strengthening of the ACC could have thermally isolated Antarctica (thus forcing the glaciation) and enhanced CO<sub>2</sub> drawdown through increasing precipitation on land (silicate weathering) (Straume et al., 2022). In addition, the EOT-1 event corresponds to a period of low summer insolation, which allowed ice sheets to persist during the summer in some places, and eventually spread over the entire Antarctic continent (DeConto & Pollard, 2003; Ladant et al., 2014).

The environmental impacts of climate change at the EOT are well-documented in the marine realm, and generally show cooling and increased variability across the globe (Lear et al., 2008; Pearson et al., 2008; Liu et al., 2009; Bohaty et al., 2012; Hutchinson et al., 2021; Toumoulin et al., 2022). Environmental impacts tend to be more heterogeneous in continental basins, largely due to the high variability of climate systems affecting continents (Hutchinson et al., 2019; Tardif et al., 2021; Toumoulin et al., 2022). Although various studies report evidence of cooling, aridification, increased seasonal climatic contrast (e.g., decrease in cold month mean temperature and increased aridity; Ivany et al., 2000; Mosbrugger et al., 2005; Dupont-Nivet et al., 2007; Eldrett et al., 2009; Utescher et al., 2015; Page et al., 2019; Hutchinson et al., 2021), and/or biotic turnovers (e.g., Hooker et al., 2004) on continents during the EOT, some do not show any significant climatic changes (Kohn et al., 2015; Zanazzi et al., 2015). These differences potentially provide information relating to the mechanisms and impacts of the EOT, but they remain poorly-documented and quantified.

This study focuses on western Eurasia, which is affected by various climate systems during the Eocene and Oligocene. In western Eurasia, the westerly-dominated moisture source may have been modulated by a proto-Atlantic Meridional Overturning Circulation (AMOC; Abelson & Erez, 2017) or affected by tectonically driven reorganization of the Arctic circulation associated with the EOT (Coxall et al., 2018; Straume et al., 2022). Several studies across Eurasia suggest that the decrease in continental temperatures was particularly pronounced in winter,

leading to a stronger seasonal temperature contrast that may have driven the well-documented biotic turnovers (e.g., Grande Coupure; Hooker et al., 2004; Mosbrugger et al., 2005; Eldrett et al., 2009; Utescher et al., 2015; Tardif et al., 2021). Furthermore, recent studies have suggested an increase in the sensitivity of climate to orbital variations across the EOT. In the Rennes Basin (France), lacustrine deposits record successive facies shifts before and after the EOT, with strengthening of the eccentricity and precession expressed in the cyclostratigraphical record (Boulila et al., 2021). This can be compared to cyclostratigraphical investigations in north-eastern Tibet, which were affected by westerlies, showing the sedimentary cycles were dominated by eccentricity prior to the EOT, and that a clear change occurred at the Oi-1 event, after which the cycles were paced by a combination of eccentricity, obliquity, and precession (Ao et al., 2020), suggesting a continental-wide increase of the sensitivity of climate to orbital variations. Increased variability and climatic seasonal contrast need to be better established and documented across Eurasian regions to better-assess potential driving mechanisms such as polar amplifications, increased Intertropical Convergence Zone (ICTZ) shifts, proto-AMOC and land-sea interactions in response to continentalization, and aridification (Abelson & Erez, 2017; Tardif et al., 2021).

Further documenting the impacts of climate change during the EOT in continental settings of western Eurasia is important as it improves our ability to assess the behavior of climate systems through major atmospheric CO<sub>2</sub> shifts, and to contextualize subsequent environmental changes. An opportunity to study these changes and to investigate climate dynamics through the EOT in a mid-latitude continental setting is provided by the rich sedimentary record of the Upper Rhine Graben (URG) rift system, which is the focus of this study.

The URG is composed of several sub-basins that have accumulated continental lacustrine sediments, and epicontinental marine strata during the middle Eocene to late Oligocene (Berger et al., 2005; Simon et al., 2021). The Mulhouse Basin, located in the south of the URG (Figure 1), is characterized by a large accumulation of predominantly lacustrine mudstones and evaporites (e.g., gypsum, anhydrite, halite, sylvite, and carnallite) of the "Zone Salifère Inférieure" (Lower Salt Zone), "Zone Salifère Moyenne" (Middle Salt Zone), and "Zone Salifère Supérieure" (Upper Salt Zone) stratigraphic formations (Blanc-Valleron, 1990; Figure 2). Such evaporitic basins are known to be particularly sensitive to climatic changes (Tanner, 2010). Past investigations in the URG suggested an increase in the seasonal climatic contrast at the base of the "Sel III" (Salt III) stratigraphic unit of the Mulhouse Basin, based largely on palynological changes (Schuler, 1988). It was also suggested that the Eocene-Oligocene boundary is represented at a certain depth within the Sel III, again largely on the basis of biostratigraphic studies and stratigraphic correlations (Grimm et al., 2011). However,

large uncertainties remain concerning the chronology, and new constraints are required to improve the chronostratigraphy and characterization of environmental change. So far, most of the information comes from palynological studies that show climate changes across the sedimentary formations (Figure 2; Schuler, 1988). Climatic conditions were subtropical with a short or nonexistent dry season through the "Zone Salifère Inférieure". Subtropical/mediterranean conditions existed through the "Zone Salifère Moyenne" (suggesting the appearance of a long dry season and thus increased seasonal climatic contrast). A drastic change in climate occurred into a dry and moderately warm mediterranean-type climate grading upwards into further temperate conditions throughout the "Zone Salifère Supérieure". However, interpretations of the rich sedimentary facies expressed in the records remain rudimentary and have not been directly compared to the climate forcing mechanism attributed to the EOT.

Seasonality refers to the annual cycles of temperature and precipitation (Kwiecien et al., 2022) and is a key phenomenon to document in the scope of EOT studies. Seasonality of temperature refers to the amplitude between the temperature maxima and minima, and seasonality of precipitation refers to the amplitude and temporal distribution of precipitation (Kwiecien et al., 2022). While isotopic and palynological investigations (Ivany et al., 2000; Eldrett et al., 2009) and numerical modeling results (Toumoulin et al., 2022) suggest an increase in seasonal climatic contrast at the EOT, marked by a fall in cold month mean temperature and higher aridity, it remains to be documented from specific changes in sedimentary facies and structures, and forcing mechanisms remain unidentified. The URG is therefore an excellent site to investigate the impacts of the EOT as it contains several Eocene-Oligocene lacustrine sequences. Furthermore, prior palynological investigations report an increase in the seasonal climatic contrast at the base of the "Sel III" unit, which is marked by the onset of a long dry season (Schuler, 1988), reinforcing the need for such a study. In this paper, we investigate the sedimentary record of the URG, with the aim of providing insights into potential seasonality contrast changes across the EOT by identifying the development of thinly-bedded cycles and associated sedimentological markers of seasonality.

## 2. Geological setting

Thanks to its rich underground resources (e.g., petroleum, potash, and geothermal brines), the structure, stratigraphy, and sedimentary record of the URG have been widely accessed through seismic imaging, drilling, coring, and borehole petrophysical logging over the past half century (Maikovsky, 1941; Sittler, 1965; Schuler, 1988; Blanc-Valleron, 1990; Roussé, 2006). The URG is an intracontinental rift system that contains several middle Eocene to late Oligocene sub-basins (e.g., Mulhouse, Sélestat, and Strasbourg basins), which are separated by structural swells (e.g., Colmar and Erstein). It is part

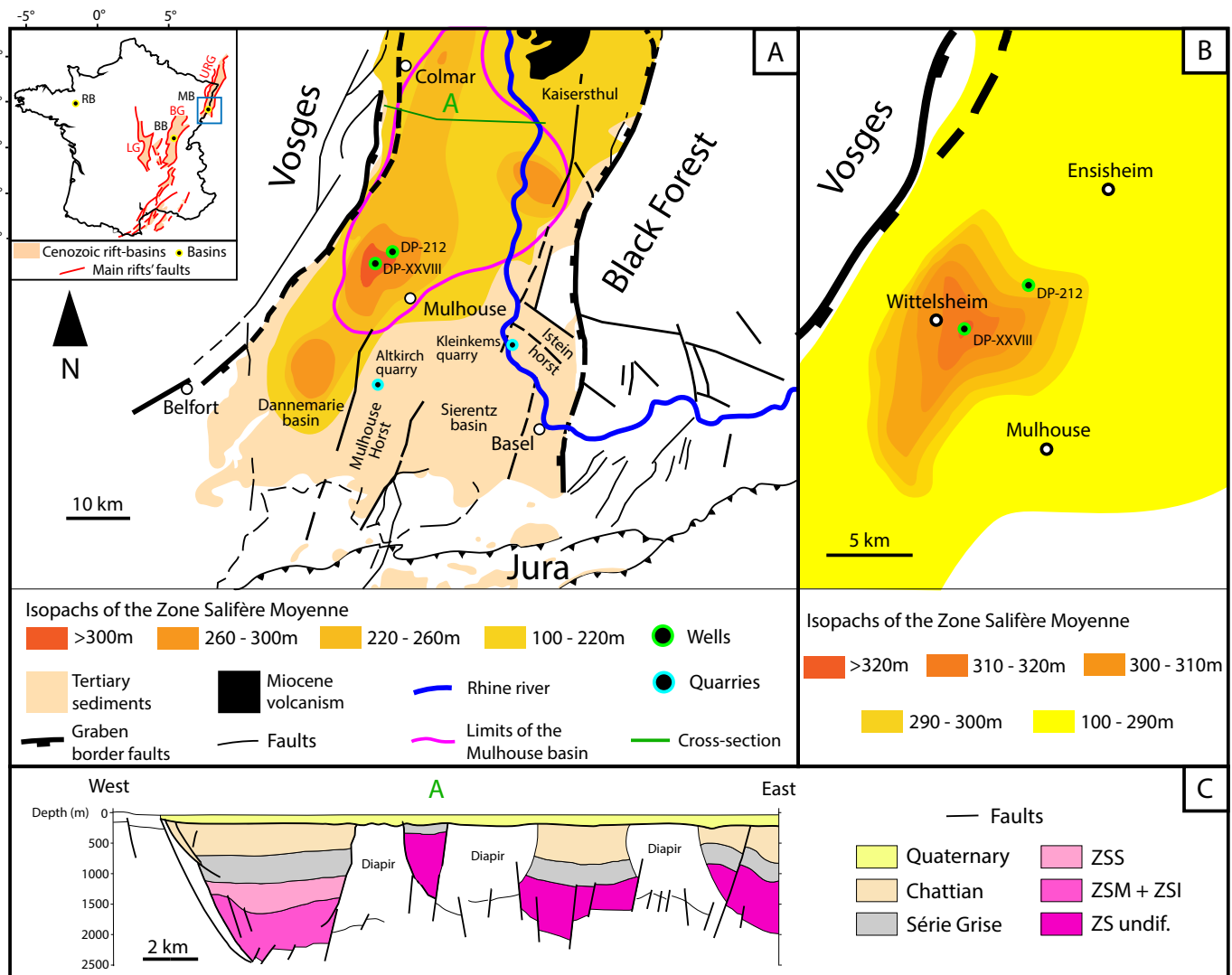


**Figure 1** | Localization map and geological structure of the southern Upper Rhine Graben. (A) Study area and details of the southern Upper Rhine Graben, with the isopachs of the "Zone Salifère Moyenne", after Blanc-Valleron (1990), Roussé (2006), and the French geological map. (B) Detailed isopachs of the "Zone Salifère Moyenne" in the Mulhouse Basin near the DP-XXVIII well, after Blanc-Valleron (1990). (C) Geological cross-section across the upper part of the Mulhouse Basin, showing the classic graben structure and occurrence of huge salt diapirs (after Roussé, 2006). URG = Upper Rhine Graben, MB = Mulhouse Basin, BG = Bresse Graben, BB = Bourg-en-Bresse Basin, LG = Limagnes Graben, RB = Rennes Basin, ZSS = Zone Salifère Supérieure, ZSM = Zone Salifère Moyenne, ZSI = Zone Salifère Inférieure, undif. = undifferentiated.

of the European Cenozoic Rift System (ECRS), which extends across ~1,100 km from the Mediterranean to the North Sea. The ECRS formed through the reactivation of Hercynian fracture systems that was induced by the continental collisions of the Alpine and Pyrenean orogens (Schumacher, 2002; Dèzes et al., 2004; Edel et al., 2007). The Tertiary sediments of the URG unconformably overlie the Mesozoic-aged Germanic Basin sediments (e.g., Buntsandstein, Muschelkalk, Keuper, Lias, and Dogger), which cover the crystalline Paleozoic basement (Aichholzer, 2019).

The Mulhouse Basin is located in the southern part of the URG (Figure 1A), and is delimited by two border faults, with large salt diapirs present in some localities (Figure 1C). The basinal infill is characterized by evaporites (e.g., anhydrite, gypsum, halite, sylvite, and carnallite), which alternate with anhydritic mudstones and carbonates (Blanc-Valleron, 1990). The mudstones primarily consist

of marlstones composed of micrite and clay to silt-sized lithogenic grains, sometimes with organic matter (Blanc-Valleron, 1990). The nomenclature of the Mulhouse Basin's sedimentary fill was first defined by Förster (1911), before being revised by Maïkovsky (1941), Courtot et al., (1972), and Blanc-Valleron (1990). The southwestern part of the Mulhouse Basin forms the main depocenter (Figure 1A, B). The "Sel III" unit and "Zone Salifère Supérieure" formations, separated by the "Zone Fossilifère" unit, consist of cyclic meter-thick to decimeter-thick mudstone-evaporite alternations (Figure 2). In the lowermost part of the "Zone Salifère Supérieure", these alternations have been interpreted as being induced by precession (Blanc-Valleron et al., 1989) based on Sediment Accumulation Rates (SARs) inferred from the finely-laminated mudstones that have been interpreted as varves (Kühn & Roth, 1979).

### 3. Material and methods

#### 3.1. Rock samples and documentation

From 1949 to 1951, a borehole (DP-XXVIII; 1948.6 m) was drilled into Quaternary, Tertiary, and Jurassic sedimentary successions by the Mines Domaniales de Potasse d'Alsace (MDPA) for exploration and production objectives. The isopach maps of the "Zone Salifère Moyenne" (Figure 1) (Blanc-Valleron, 1990) reveal that the DP-XXVIII well captures the depocenter of the Mulhouse Basin, suggesting maximum sedimentary continuity. Core samples from this well (at a scale averaging a sample every few meters) were made accessible by the Musée d'Histoire Naturelle et d'Ethnographie of Colmar for the purposes of the current study (see supplementary files). The preservation of several samples is rather poor, and almost all halite samples are re-precipitated, however most mudstone samples are in good condition. The original detailed lithological description of the DP-XXVIII well by the MDPa was made accessible by the KALIVIE museum (Wittelsheim; MDPa, 1960). The arranged dataset was amalgamated into a sedimentary log of the well (see supplementary files). In addition, laminated rock samples were collected from the "Zone Fossilifère" unit exposed in both the Altkirch and Kleinkems quarries (Figure 1A).

#### 3.2. Sediment macro- and micro-facies analysis

Micro-facies descriptions were performed on both thin and thick sections from selected and suitable samples of the DP-XXVIII well, and the Altkirch and Kleinkems quarries. Both macro- and micro-facies descriptions, as well as thin and thick section photographs were realized using a Leica M205 C stereo microscope. A total of 203 core samples have been investigated and their positions in the sedimentary log of the well are shown in the supplementary file (Figure S1).

#### 3.3. Micro X-Ray fluorescence scanning

Micro X-Ray Fluorescence ( $\mu$ -XRF) analyses were performed on thin and thick sections using a Bruker M4 Tornado spectrometer at the Institut Terre & Environnement of Strasbourg. The maximum resolution of 20  $\mu$ m was used in order to achieve the best representative elemental counts for each lamina. The spectrometer settings were set on a voltage of 50 kV, ampere ratings of 400  $\mu$ A, and the analyses were performed under vacuum conditions (2 mbar). We selected a set of representative elements to determine the relative changes in detrital input (aluminum, silica potassium, titanium, iron – Al, Si, K, Ti, Fe) and chemogenic or diagenetic deposition (calcium, strontium, sulfur – Ca, Sr, S) (Boës et al., 2011; Davies et al., 2015). Elemental contents are reported as log-ratios in order to avoid closed-sum constraints (Weltje et al., 2015).

#### 3.4. Scanning electron microscope

Scanning Electron Microscope (SEM) images and local chemical analyses were performed on a thin section and on a rock sample from the DP-XXVIII well to document the chemistry and microstructure of minerals using a VEGA TESCAN machine.

#### 3.5. Spectral analysis

Spectral analysis was performed on the Gamma-Ray (GR) series from the "Sel V" unit of the DP-212 well to test the hypothesis of orbital forcing of the meter-thick to decameter-thick mudstone-evaporite alternations. The GR was measured by the MDPa through Schlumberger electrical logging and records the natural radioactivity of the sedimentary record. The GR series was interpolated, linearly detrended, and normalized using Acycle's "normalize" function (z-scoring, Li et al., 2019). Sedimentary cycles and their evolution were studied using the Multi-Taper Method applying  $2\pi$ -tapers with red-noise modeling ( $2\pi$ -MTM analysis; robust AR(1) test) to detect statistically significant sedimentary cycles (Thomson, 1982; Mann & Lees, 1996), the Evolutive Fast Fourier Transform (EFFT) to document the evolution of sedimentary cycles through depth (Weedon, 2003), and Taner band-pass filters to isolate specific broadbands (Taner, 2000). These methods were performed using the Acycle software (v2.3.1; Li et al., 2019). The classical AR(1) test was also performed (Priestley, 1981).

## 4. Results

### 4.1. DP-XXVIII well

#### 4.1.1. Synthetic sedimentary log

The detailed sedimentary log of the DP-XXVIII well (see supplementary files) was produced based on the written description of the sedimentary successions made by the MDPa in the mid-20<sup>th</sup> century (MDPa, 1960), which we then synthesized (Figure 2). Here, we focus on the three zones as defined by Blanc-Valleron (1990) to investigate sedimentary changes across the EOT.

The "Zone Salifère Inférieure" is divided into four units (from base to top): the "Marnes à Limnées I" (Limnea Marls I) unit (thickness: 155 m) consists of massive mudstones alternating with centimeter to meter thick, bedded to nodular anhydrite layers. The "Sel I" (Salt I) unit (thickness: 165 m) is a massive halite formation with rare intercalations of centimeter-thick mudstone and anhydrite layers. The halite is described as made up of centimeter-thick crystals forming chevrons (MDPa, 1960), which could correspond to bottom nucleated beds of coarse growth-aligned crystals at the sediment/water interface. The lithology of the "Marnes à Limnées II" (Limnea Marls II) unit (thickness: 84 m) is similar to the "Marnes à Limnées I", followed by the "Sel II" (Salt II) unit (thickness: 117 m), which has a similar

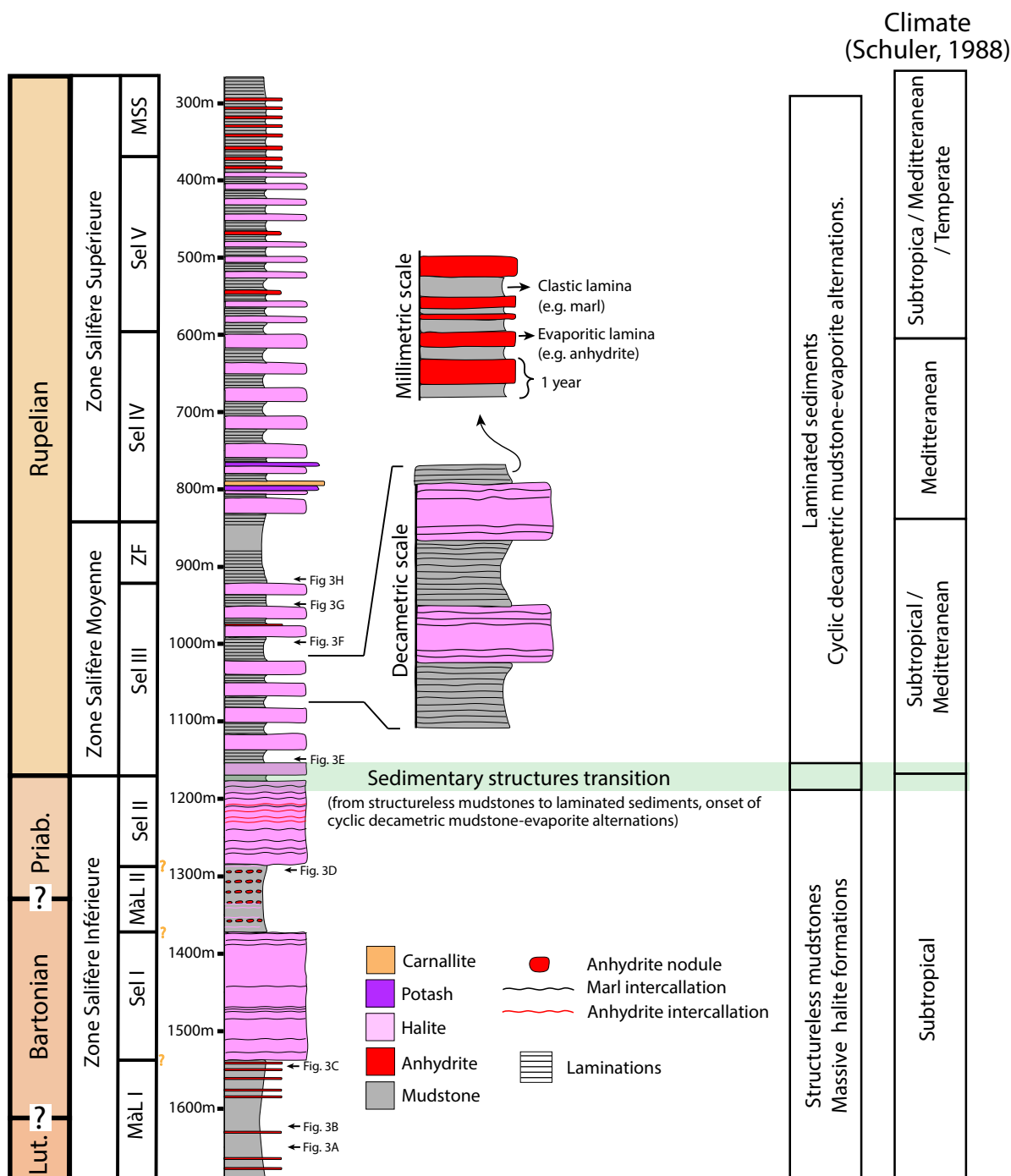


**Figure 2** | Synthetic log of the sedimentary succession of the Mulhouse Basin's formations through a segment of the DP-XXVIII well, with the paleoclimatic observations inferred from palynology (Schuler, 1988). The chronostratigraphy is based after Grimm et al. (2011) and Châteauneuf & Ménillet (2014), and the Eocene-Oligocene boundary is placed according to the correlations presented in this paper. The thickness of the mudstone-evaporite alternations of the "Sel III" and "Zone Salifère Supérieure" are exaggerated. MâL I = Marnes à Limnées I, MâL II = Marnes à Limnées II, MSS = Marnes sans Sel.

lithology as the "Sel I" unit, contains substantially more intercalations of centimeter-thick to meter-thick mudstone and anhydrite beds.

The "Zone Salifère Moyenne" comprises two units (from base to top). The "Sel III" unit (thickness: 249 m) consists of cyclic decimeter-thick alternations of laminated mudstones and massive halite beds (their average thickness is ~12.6 m). The laminated mudstones of this unit are often described as made up of millimeter-thick laminae (MDPA, 1960). The overlying "Zone Fossilifère" (Fossiliferous Zone) unit (thickness: 80 m) is a thick

mudstone formation attributed to a transgression event that flooded the whole URG during the early Rupelian (Berger et al., 2005; Pirkenseer et al., 2010) and consists of laminated mudstones with occasional dolomite and anhydrite layers.

The "Zone Salifère Supérieure" is composed of three units (from base to top). The "Sel IV" (Salt IV) unit (thickness: ~246 m) is made of cyclic decimeter-thick mudstone-halite alternations (average thickness of ~12.4 m). The mudstone beds of these alternations are mostly laminated. Two meter-thick intervals of centimeter-thick halite and sylvite

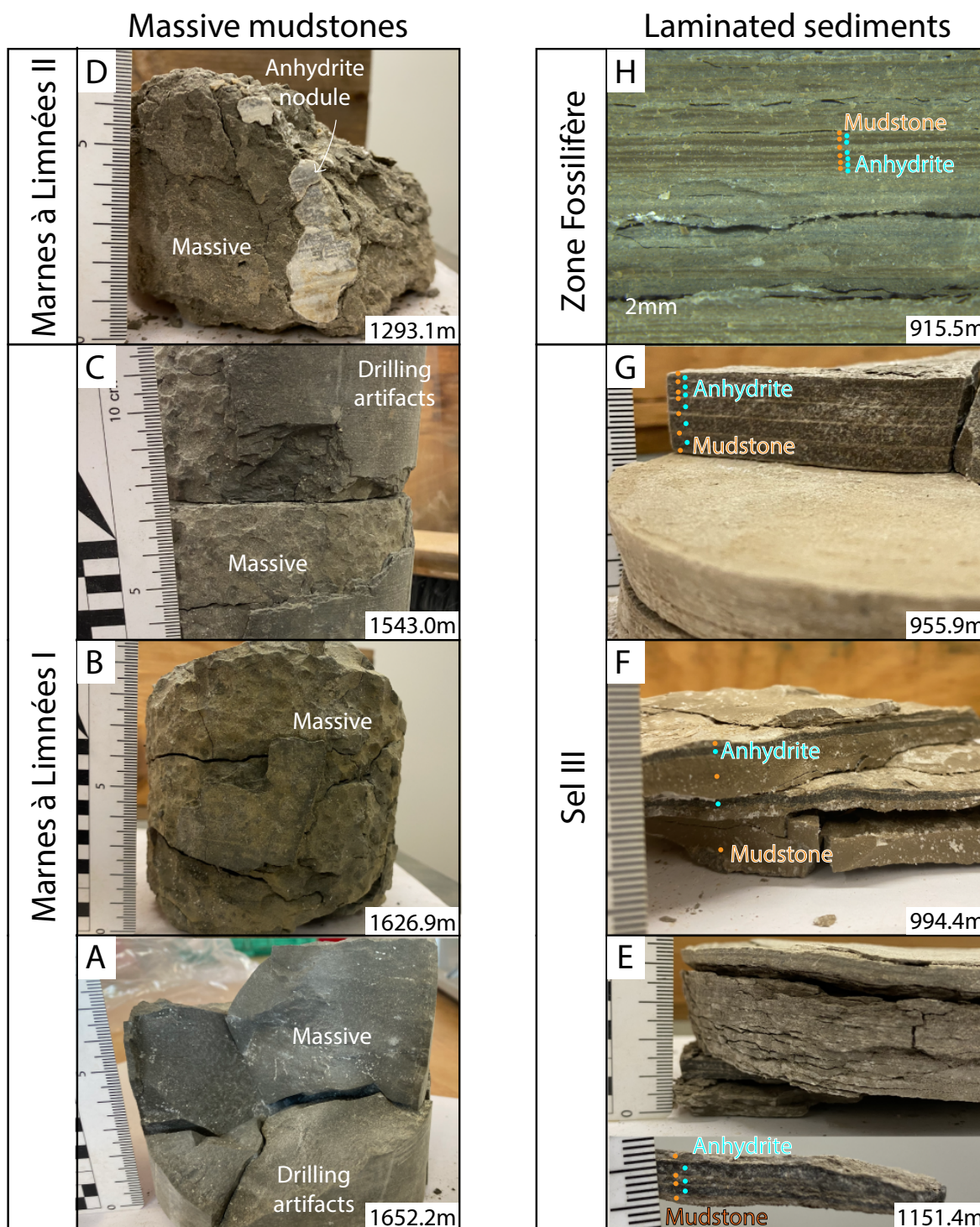


**Figure 3** | Macro-photographs of core samples from the DP-XXVIII well. (A, B, C, D) Massive mudstones with conchoidal fractures. Coring artifacts from the drill machine are not to be mistaken with laminations. (E, F, G, H) Laminae consisting of mudstone (light-colored laminae) and anhydrite (dark-colored laminae) couplets.

alternations (commonly draped by anhydritic marlstones and dolomitic carbonates), with occasionally interbedded centimeter-thick laminated boundstones, are identified at the bottom of the formation. A 1.2 m thick carnallite bed is located at the top of the lower potash seam. The “Sel V” unit (thickness: ~227 m) is made of cyclic meter-thick alternations of halite (or anhydrite) and mudstone beds, which average ~8.3 m in thickness. The following “Marnes sans Sel” (Salt-free Marls) unit (thickness: ~106 m) consists of cyclic meter-thick mudstone-anhydrite alternations (with an average thickness of ~5.6 m). The mudstone beds of these alternations appear mostly laminated, yet the

upper ~45 m is composed of a thick mudstone section without any observable sedimentary alternations. Overall, the “Zone Salifère Supérieure” is characterized by its cyclic meter-thick to decimeter-thick mudstone-evaporite alternations, where the mudstones are mostly laminated, and by the presence of two potash seams in its lowermost part.

Across the three formations, the mudstones can be divided into two main groups according to the absence or presence of sedimentary structures: (1) massive and (2) laminated mudstones. Massive mudstones are common in



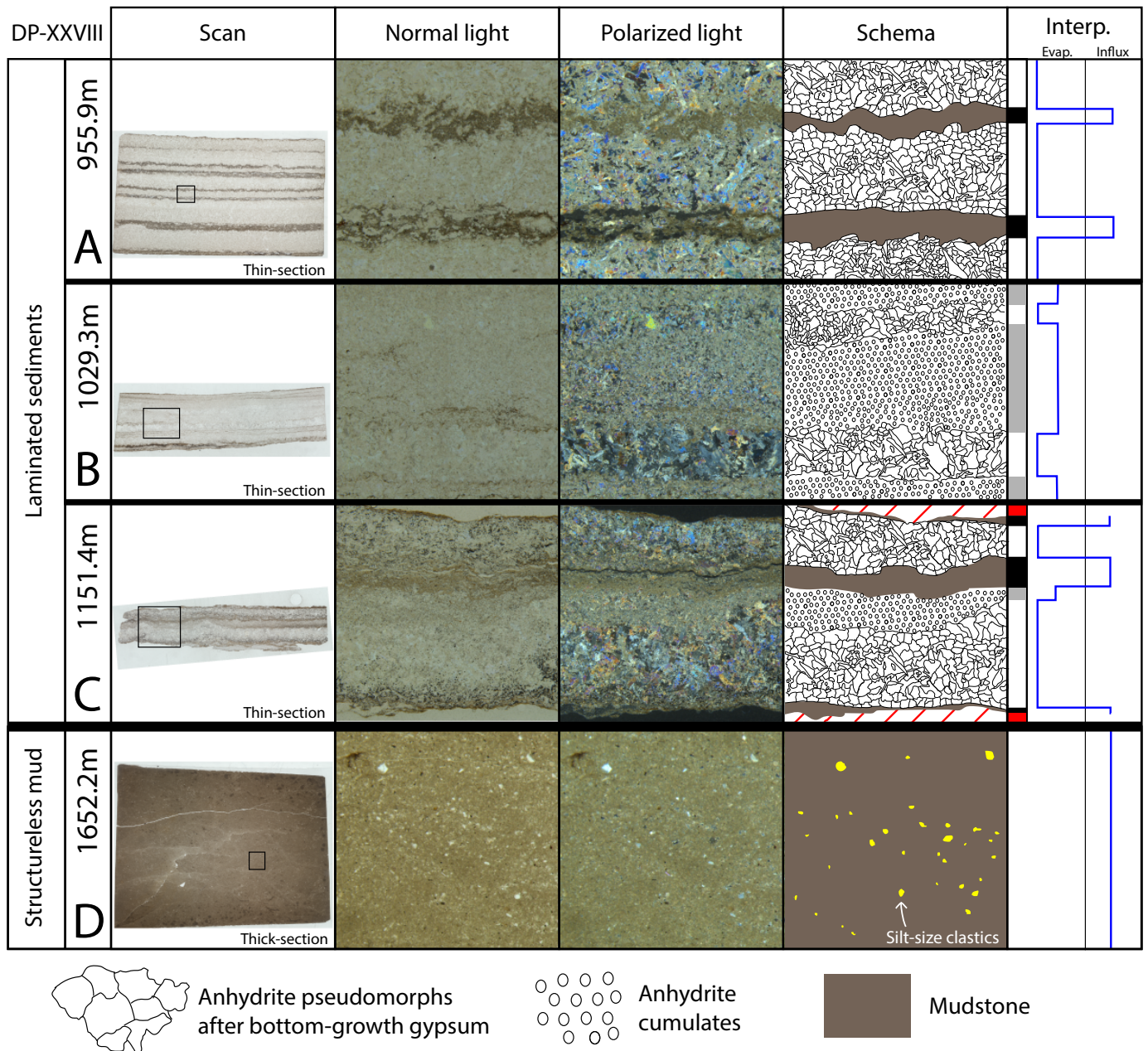


**Figure 4** | Thin sections of laminated sediments, and thick section of a massive mudstone, from the DP-XXVIII well. (A) Laminated sediments made of couplets of mudstones and anhydrite pseudomorphs after bottom-growth gypsum (955.9 m). (B) Laminated sediments made of couplets of anhydrite pseudomorphs after bottom-growth gypsum and anhydrite cumulates with some very thin mudstone drapes (1029.3 m). (C) Laminated sediments made of couplets of mudstone, anhydrite pseudomorphs overlying bottom-growth gypsum, and anhydrite crystals (1151.4 m). (D) Massive mudstone consisting of silt-sized clastic grains in a micrite matrix (1652.2 m).

the "Zone Salifère Inférieure", where very few laminated mudstones have been described (MDPA, 1960). In the lowermost "Zone Salifère Moyenne", a clear facies change occurs with the appearance of laminated mudstones that make-up most of the mudstones up to the top of the "Zone Salifère Supérieure". The seemingly cyclic decimeter-thick mudstone-evaporite alternations appear at the same depth as the finely-laminated mudstones and remain a predominant feature up to the uppermost "Zone Salifère Supérieure". However, evaporites are scarce in the "Zone Fossilifère", even though laminated mudstones remain prevalent. To sum up, the study of the original description of the DP-XXVIII well (MDPA, 1960) reveals that both the millimeter-thick laminae and the recurrent meter-thick to decimeter-thick mudstone-evaporite alternations appear at the bottom of the "Sel III" (depth: 1158 m) and

are found up to the uppermost part of the "Zone Salifère Supérieure" (depth: 312 m). The mudstone-evaporite alternations become thinner upward in the section, from ~12.6 m in the "Sel III" to ~5.6 m in the "Marnes sans Sel", suggesting a gradual decrease in SARs.

#### 4.1.2. Macro-facies of the core samples

The three main lithologies represented in the DP-XXVIII core are mudstone, halite, and anhydrite. Macro-facies observations of the mudstones are in accordance with the available description (MDPA, 1960; Figure 3). The massive mudstones are predominant in the "Zone Salifère Inférieure", whereas the laminated mudstones are predominant in the "Zone Salifère Moyenne". However, a few laminated samples are present in the "Sel II" unit.

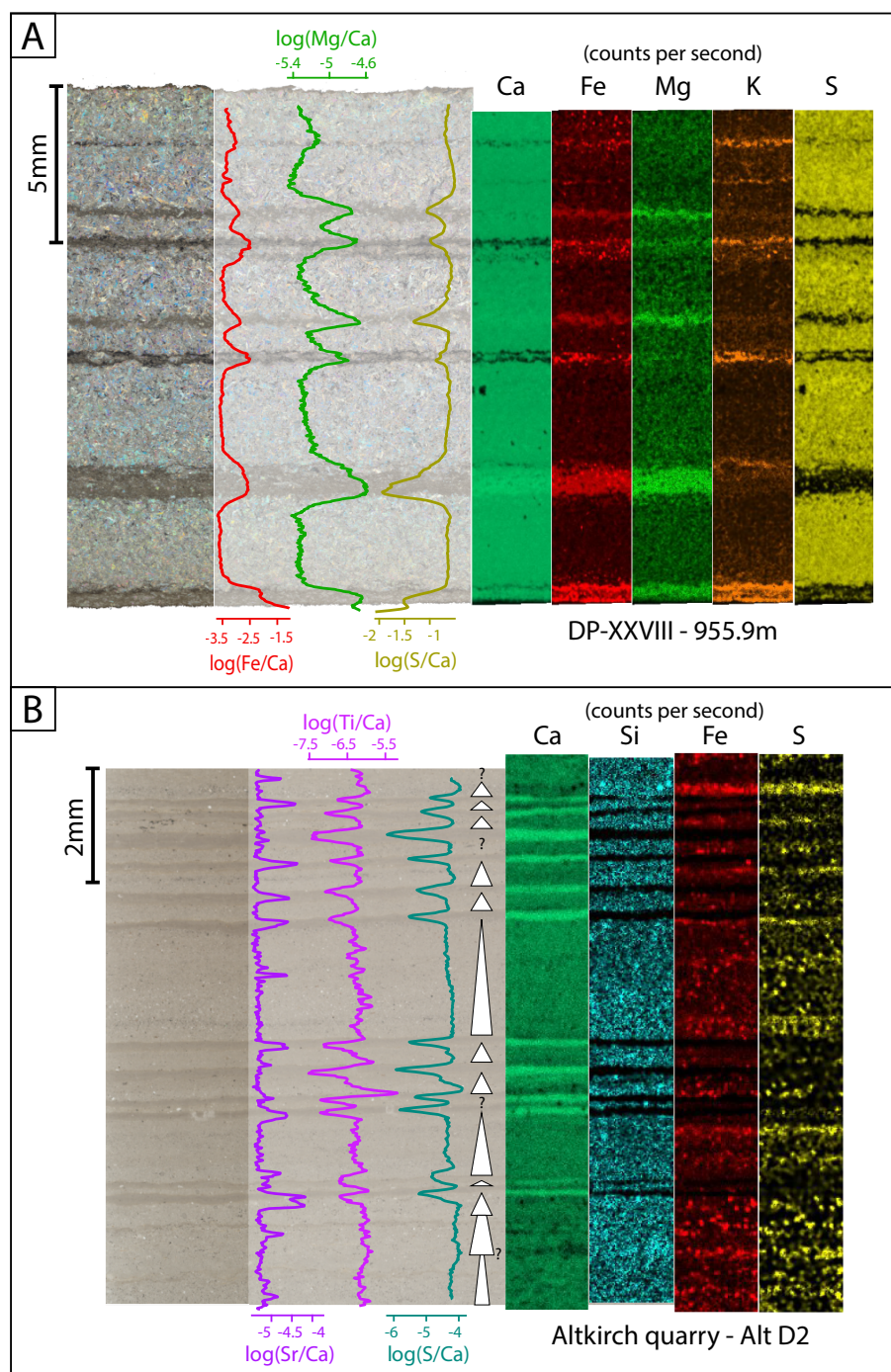


**Figure 5** |  $\mu$ -XRF analyses consisting of logarithms of specific elemental ratios and elemental mappings of the DP-XXVIII well sample, at depth 955.9 m, and of the Alt-D2 sample from the Altkirch Quarry. In the case of elemental mappings, black represents no counts per second, while the colors represent higher counts per seconds based on the intensity. The white triangles represent fining-up sequences. (A) (DP-XXVIII - 955.9 m) The  $\mu$ -XRF analyses show that the light-colored laminae are anhydrite (rich in Ca and S) and that the dark-colored laminae range from marl to dolomite due to their varying intensities of Ca and Mg. Furthermore, the elemental mappings show an enrichment in lithogenic elements (e.g., Fe, K) in the dark-colored laminae, suggesting their detrital nature. (B) (Altkirch Quarry - Alt D2) The  $\mu$ -XRF analyses show that the dark-colored laminae are rich in Ca, enriched in Sr, and completely devoid of lithogenic elements, suggesting an evaporitic nature. Inversely, the light-colored laminae are enriched in lithogenic elements (e.g., Si, Ti, Fe), which suggests a detrital nature, further demonstrated by fining-up sequences.

The laminated mudstones consist of millimeter-thick laminae, several of which are made of couplets of dark- and light-colored laminae, especially moving upward from the base of the "Sel III" unit. At the macroscopic scale, the dark-colored laminae are primarily composed of anhydrite, while the light-colored laminae are mainly composed of siliciclastic mud (Figure 3E-H). While some are very finely laminated (e.g., Figure 3E, G), others exhibit thicker layers (e.g., Figure 3G). At the microscopic (thin

section) scale, the color pattern of these laminae is the opposite, with anhydrite laminae being light-colored and mudstone laminae being dark-colored (Figure 4).

The halite core samples have been impacted by recrystallization, preventing proper identification of the depositional environment. The anhydrite either forms centimeter-thick elongated to sub-rounded nodule beds, with vestigial

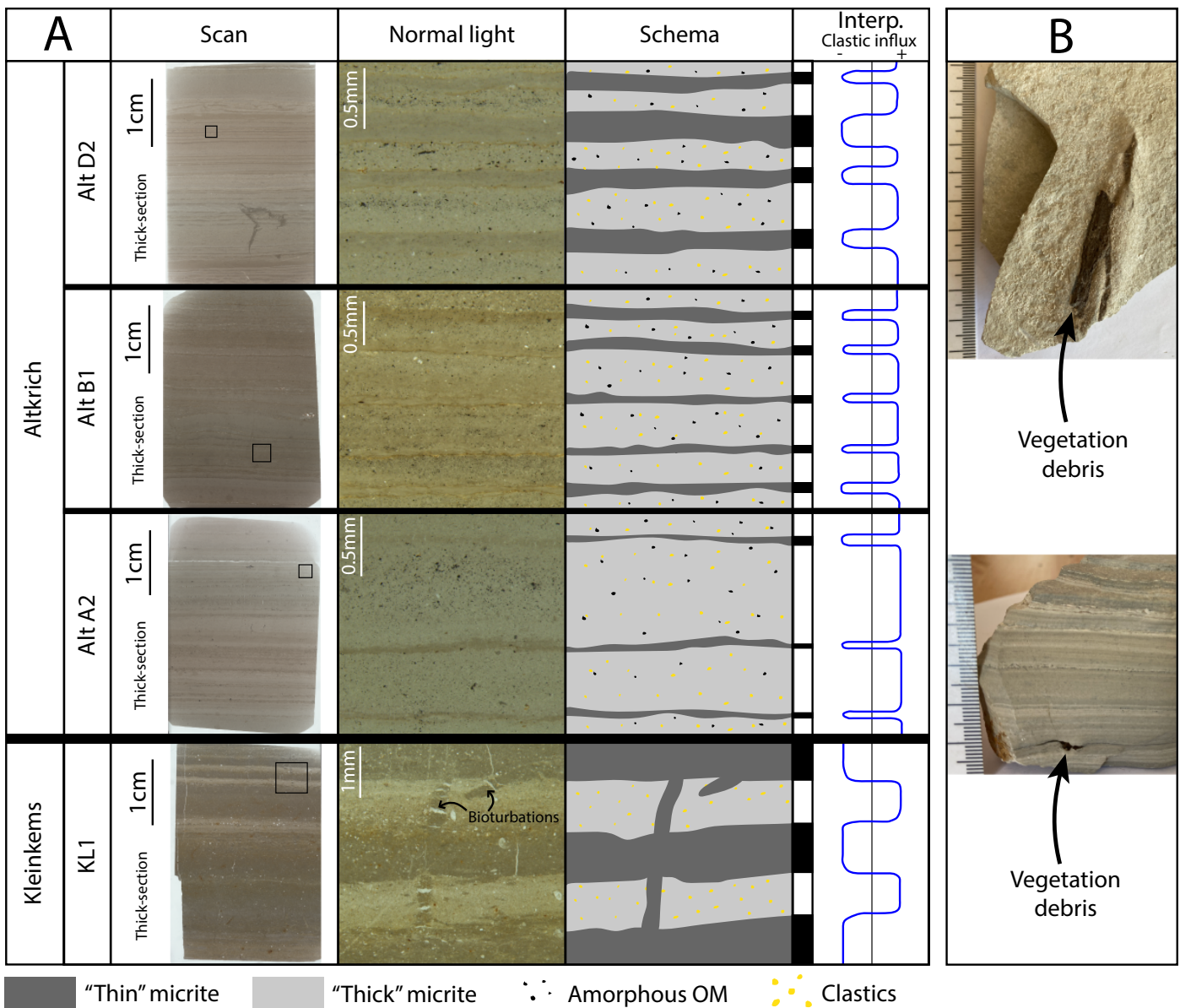


**Figure 6** | (A) Thick sections of laminated sediments from the Altkirch and Kleinkems quarries ("Zone Fossilifère"). (Alt D2, Alt B-1, and Alt-A2) Laminated sediments made of couplets of thin micrite crystals (dark-colored laminae) and thicker micrite crystals, amorphous organic matter, and detrital grains (light-colored laminae). (KL1) Laminated sediments similar to those from the Altkirch Quarry, but without amorphous organic matter, and with shells across the laminae. (B) Macro-photographs of laminated sediments from the Altkirch Quarry containing macroscopic vegetation debris.

bottom-growth structures encompassing marlstone, or layers.

## 4.2. Laminated sediments of the southern Upper Rhine Graben

### 4.2.1. Depocenter (DP-XXVIII well)

In the "Zone Salifère Moyenne", 61 out of 68 mudstone samples are laminated (see supplementary files). Observation of the samples under the microscope reveals repetitive couplets and triplets of dark- and light-colored laminae (Figure 4). The 955.9 m sample consists of repetitive couplets of anhydrite pseudomorphs derived from bottom-growth gypsum (light-colored laminae) and marlstones (dark-colored laminae). The 1151.4 m sample contains an additional fine-grained (~30  $\mu\text{m}$ ) anhydrite lamina (cumulates). Dark-colored laminae contain

homogenous and massive clay-sized sediments. Some of the laminae are black, suggesting an enrichment in organic matter as indicated by the SEM measurements. In the case of the 1029.3 m sample, the sediments are typified by two couplets of anhydrite pseudomorph laminae, overlain by of discontinuous draping clay, without significant dissolution surfaces. Typically, gypsum pseudomorphs form as bottom-nucleated crystals that grown on the lake floor when brine is saturated with respect to sulfates (Warren, 2016).

The elemental geochemistry analysis of the 955.9 m sample shows that the light-colored laminae are enriched in Ca and S, which track the presence of anhydrite, which is also inferred from microfacies observations (Figure 5A). The dark-colored laminae are enriched in Fe, Mg, and K, which indicates they are primarily composed of detrital siliciclastic minerals (clay). The dark-colored laminae are

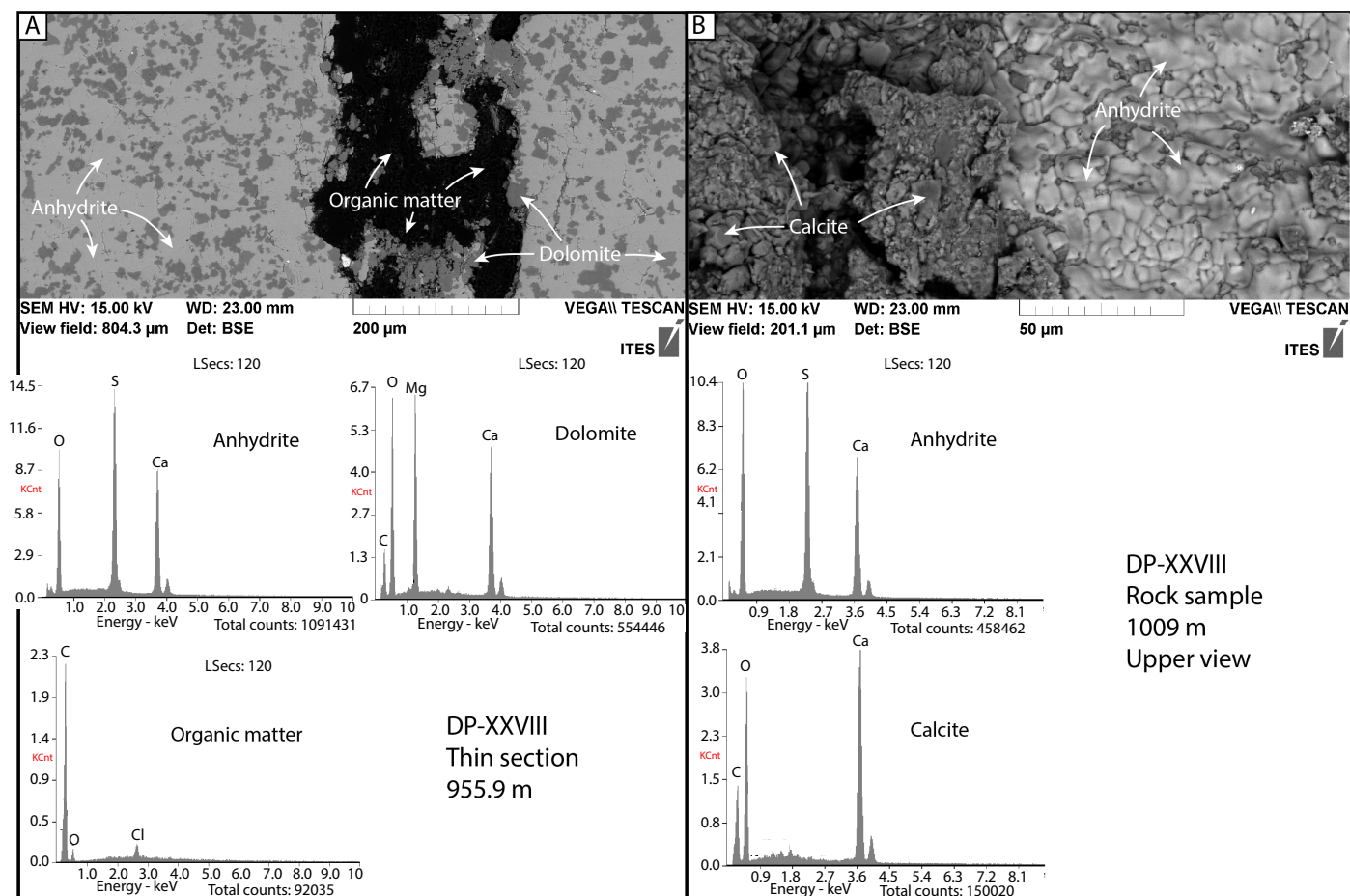


**Figure 7** | SEM images and localized chemical analyses of a part of the (A) thin section at 955.9 m depth and (B) sample at 1009 m depth.

enriched in Mg (high Mg/Ca ratios) and can therefore contain dolomite ( $\{Ca,Mg\}CO_3$ ) which amount might depend on the presence of Ca (see element maps, Figure 5A). The S content is generally low in dark-colored laminae (low S/Ca ratios), which confirms the absence of anhydrite, but enrichments of S are occasionally observed. This can possibly be attributed to the presence of diagenetic processes that induce pyrite precipitation ( $FeS_2$ ) (e.g., the third mudstone laminae starting from the bottom, Figure 5A). Similar elemental compositions were found for the samples at 1029.3 m and 1151.4 m depth (see supplementary files), which suggest similar genesis of the sediments as the sample at a depth of 955.9 m.

#### 4.2.2. Altkirch Quarry

The laminated sediments from the lowermost part of the Altkirch Quarry ("Zone Fossilifère") were first described as varves based on the repetitive nature of their dark- and light-colored laminae (Düringer, 1988; Figure 6). The dark-colored laminae are homogenous, have a constant thickness, and consist of very fine micrite crystals ( $<1 \mu m$ ). The light-colored laminae (0.15 – 2 mm thick) are composed of larger micrite crystals ( $\sim 2 \mu m$ ) and contain clastic grains, along with amorphous organic matter (Figure 6A). The Altkirch Quarry is known for its rich diversity of macrofossil taxons (e.g., fish, insects, and mollusks;

Gaudant & Burkhardt, 1984), thus a certain amount of the organic content could also be autochthonous.

Elemental analyses of the Altkirch laminated sediments (Alt D2 sample, Figure 5B) show that the dark-colored laminae are enriched in Ca and Sr, while the Si, Ti, Fe, S, and K values are higher in the light-colored laminae (Figure 5B). Several dark-colored layers also contain higher concentrations of Sr (higher Sr/Ca ratios), which potentially indicates the presence of Sr-enriched carbonates, such as aragonite or strontianite. Dark-colored layers are devoid of detrital material (low Si/Ca and Ti/Ca ratios, absence of Si and Fe in element maps), which suggests that the thin micrite crystals of the latter are chemogenic (evaporitic) rather than detrital. In light-colored layers, high levels of lithogenic elements (e.g., Si, Fe, and Ti) track the input of clastic material (e.g., quartz, and feldspars) identified in the micro-facies analysis. The detrital-rich light-colored laminae show distinct fining-upward sequences (Figure 5B), which is evidenced by decreasing log-ratio profiles of Si/Ca and Ti/Ca and decreasing grain-sizes observable on the elemental map of Si. The enrichment in both Fe and S in light-colored laminae suggests the presence of iron sulfides (e.g., pyrite). The clastic grains in the light-colored layers are encased in a micrite matrix (cement). Comparable results were found for the Alt A2 and Alt B1 samples (see Data Availability), which suggest that their laminae are similar in nature to those of the Alt D2 sample.

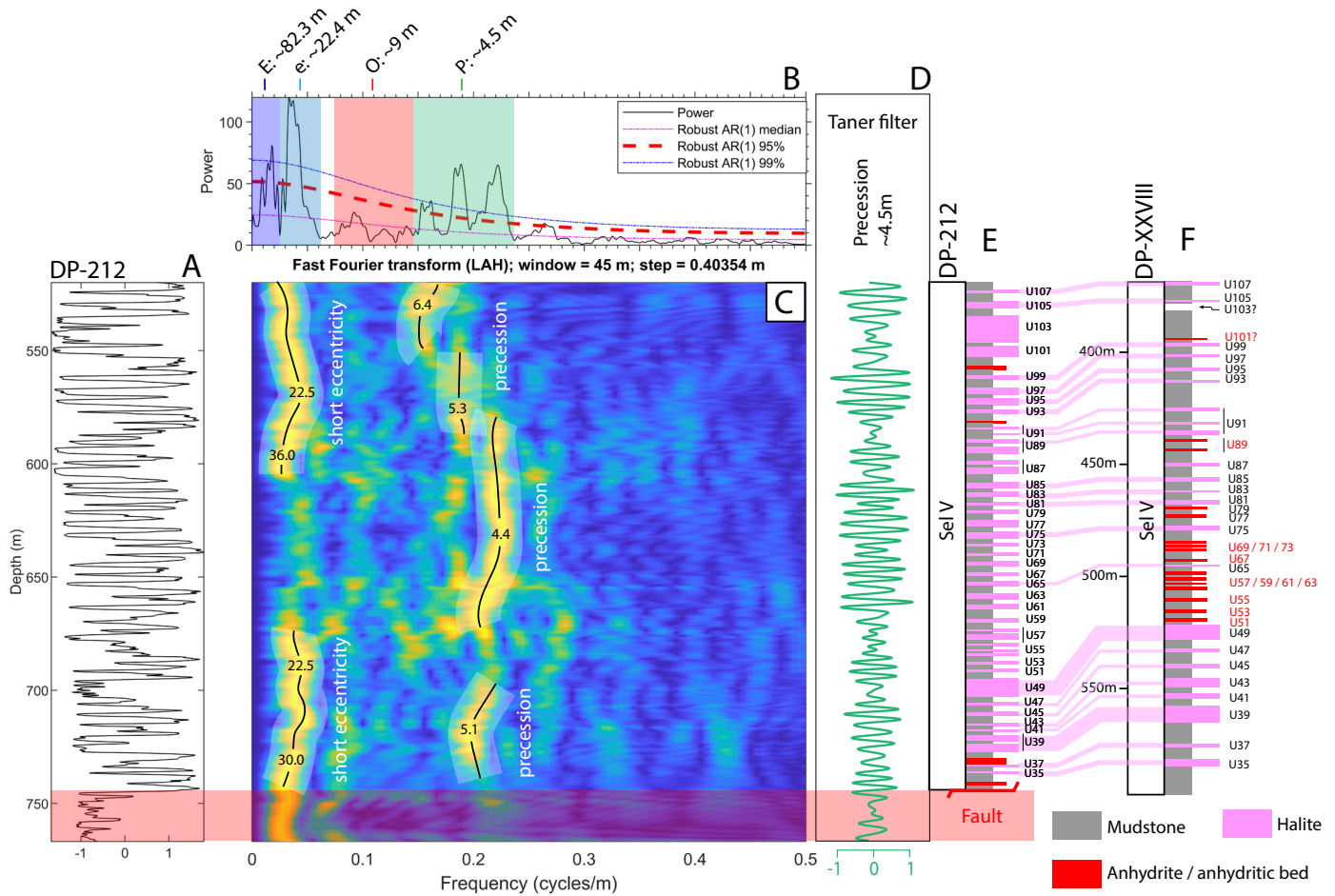


**Figure 8** | Spectral analysis results of the “Sel V” unit of the DP-212 well (“Zone Salifère Supérieure”). (A) Linearly detrended gamma-ray series (DP-212). (B)  $2\pi$ -multitaper spectrum with linearly fitted red-noise modelling. E = long eccentricity, e = short eccentricity, O = obliquity, P = precession. (C) EFFT with a sliding window of 45 m and a step of 0.40354 m. (D) Taner filter of the precession (P; 0.1459 – 0.2998 cycles/m) cycles. (E) Sedimentary log of the DP-212 well (“Sel V”). (F) The equivalent sedimentary log of the DP-XXVIII well (“Sel V”). The “U” followed by numbers are the name of each halite bed as initially established by the MDPA (Blanc-Valleron, 1990).

#### 4.2.3. Kleinkems Quarry

The laminated sample from the Kleinkems Quarry contains several successions of dark- and light-colored calcareous laminae (Figure 6). The dark-colored laminae are comparable to those from the Altkirch Quarry and are composed of homogeneous bioclastic fine-grained micrite, with randomly distributed shells. The light-colored laminae, similarly to those from Altkirch Quarry, contain a significant amount of clastic grains, but no amorphous organic matter. The  $\mu$ -XRF analysis of the KL1 sample shows similar elemental distribution as in the samples from the Altkirch Quarry (see supplementary files). However, the dark-colored Ca-rich laminae also contains some detrital material, as indicated by the presence of a few lithogenic grains.

#### 4.3. Scanning Electron Microscope

SEM images and localized chemical analyses of a part of the 955.9 m thin section shows the presence of anhydrite (light gray), dolomite (dark gray), and organic matter (black) (Figure 7A). Small dolomite patches are encased in the anhydrite. The image of the sample at depth 1009 m shows the presence of anhydrite (light gray) and calcite

(dark gray) arranged in layers (upper view) (Figure 7B). The anhydrite is characterized by high counts of Ca, S, and O; the dolomite by high counts in Ca, Mg, O, and C; the calcite by high counts in Ca, O, and C, and the organic matter by high counts in C.

#### 4.4. Spectral analysis

The  $2\pi$ -MTM analysis results of the detrended GR series (Figure 8A) of the “Sel V” unit from the DP-212 well reveals statistically significant frequency broadbands related to sedimentary cycles, with average thicknesses of 82.3 m, 22.4 m, and 4.5 m (>99% confidence level), and 9 m (> median confidence level) (Figure 8B). The broadband related to the ~4.5 m thick sedimentary cycle shows three distinct peaks. The EFFT shows that the ~22.4 m and the ~4.5 m cycle are prominent throughout the sedimentary record (Figure 8C). The Taner filter of the ~4.5 m cycle is in-phase with the large majority of the mudstone-evaporite alternations (Figure 8D, E). The classical AR(1) test shows that almost the whole signal is above the 99.9% confidence level, and that the same frequency peaks appear with the highest amplitudes, except for the ~82.3 m cycle (see supplementary files).

## 5. Interpretation and discussion

To achieve the goals of this study, we interpret and discuss in the following sections the results presented above to:

- estimate whether the observed laminae represent an annually deposited cycle (varves) and if they can thus be used as markers of seasonality;
- discern the possible mechanisms behind the cyclic sedimentation pattern of the laminae and decimeter-thick mudstone-evaporite alternations, with implication for better understanding past environmental changes;
- and to place the interpretation of this study in a wider regional scale and to discuss the implications for climatic changes across the EOT.

### 5.1. Laminated sediments and varves: nature and depositional processes

Distinguishing varves from non-annual laminated sediments is challenging for sedimentary archives beyond the radiometric time range. While the annual nature of varves in modern and recent lacustrine and marine environments can be determined using various means (Zolitschka et al., 2015), it can only be hypothesized in older geological (deep-time) records, by interpreting and comparing of petrographical and geochemical data with their modern and recent counterparts (Wilson & Bogen, 1994; Mingram, 1998). For the southern URG, we use the sedimentary records of the Dead Sea, which contain extensive evaporite deposits (Ben Dor et al., 2019), and of Chatyr Kol Lake (Kalanke et al., 2020) as sedimentary analogues, which allow us to propose conceptual models for reconstructing depositional processes.

#### 5.1.1. Distinguishing varves from laminated sediments

Lacustrine sediments, such as laminated sediments and varves, can be categorized as clastic, biogenic, or endogenic (Brauer et al., 2009; Zolitschka et al., 2015). Varves are a particular type of laminated sediments, which are defined as sedimentary layers of distinct composition, occurring as repetitive patterns that represent annual cycles (Zolitschka et al., 2015). The identification of varves is a strong indicator of local climatic seasonality. Clastic varves are formed when suspended sediment carried by seasonal runoff enters a lake with a stratified water body (Sturm, 1979). They are typically made of laminae with different grain sizes that results from distinct seasonal runoff regimes. Biogenic varves are formed when seasonality induces changes in the organic productivity of a lake, resulting in the deposition of distinct biogenic laminae (e.g., algal blooms, diatom blooms; Lake Tiefer, Germany; Dräger et al., 2017). Endogenic varves, which are often evaporitic, occur when the solubility product of a mineral compound (e.g., anhydrite, halite, and aragonite) is exceeded due to

seasonal fluctuations of evaporation and/or precipitation (e.g., the Dead Sea; Ben Dor et al., 2019). It is rare that varves are either purely clastic, biogenic, or endogenic (Zolitschka et al., 2015). The Varves Database provides an overview of many varve records and of their characteristics (Ojala et al., 2012). It should be noted that the presence of laminated sediments and varves indicates that the depositional environment prevented the development of benthic life and bioturbation. It is however beyond the scope of our study to determine whether it has been the lack of oxygen or a specific water chemistry (e.g., hypersaline waters), or a combination of the two that have rendered the lake floor uninhabitable.

#### 5.1.2. Interpretation of the fine laminations as varves and conceptual depositional model

##### 5.1.2.1. Depocenter (DP-XXVIII well)

The samples from the DP-XXVIII core display clear couplets of mudstone and anhydrite pseudomorphs after bottom-growth gypsum, with no dissolution surfaces (Figure 4, Figure 5A). We propose that the evaporites were formed through evaporation-driven brine saturation during the dry season, and that the intercalated mudstone layers (sometimes rich in organic matter) were formed due to enhanced fluvial runoff during the wet season (Figure 9). This interpretation is supported by the elemental profiles that clearly distinguish between anhydritic laminae (enriched in Ca and S) and detrital mudstone laminae (enriched in the lithogenic elements Fe and K) (Figure 5A). According to the palynological investigations and taking into account the mid-latitude position of the site, climatic conditions resembled today's Mediterranean climate throughout the "Zone Salifère Moyenne", with distinct wet (winter) and dry (summer) seasons (Schuler, 1988). Furthermore, these mudstone-anhydrite couplets are similar to varves from the late Pleistocene Lisan Formation (Dead Sea, Israel) (Ben Dor et al., 2019), which are composed of endogenic aragonite and gypsum laminae precipitating during dry summers, and detrital-rich laminae deposited during winter runoff. We therefore consider the thin mudstone-anhydrite couplets of the DP-XXVIII well as endogenic-clastic varves, comparable to those of the Dead Sea, even though processes might differ following water balance conditions.

The anhydrite pseudomorphs overlying bottom-nucleated gypsum and thin crystal (anhydrite cumulates) couplets of the 1029.3 m sample could also be varves, but these were deposited under drier conditions than the mudstone-anhydrite examples (Figure 4). The first ones are similar to seasonal temperature-driven couplets described in the Dead Sea, which are composed of alternations of coarse and fine halite or gypsum crystals (Sirota et al., 2017; Ben Dor et al., 2019).

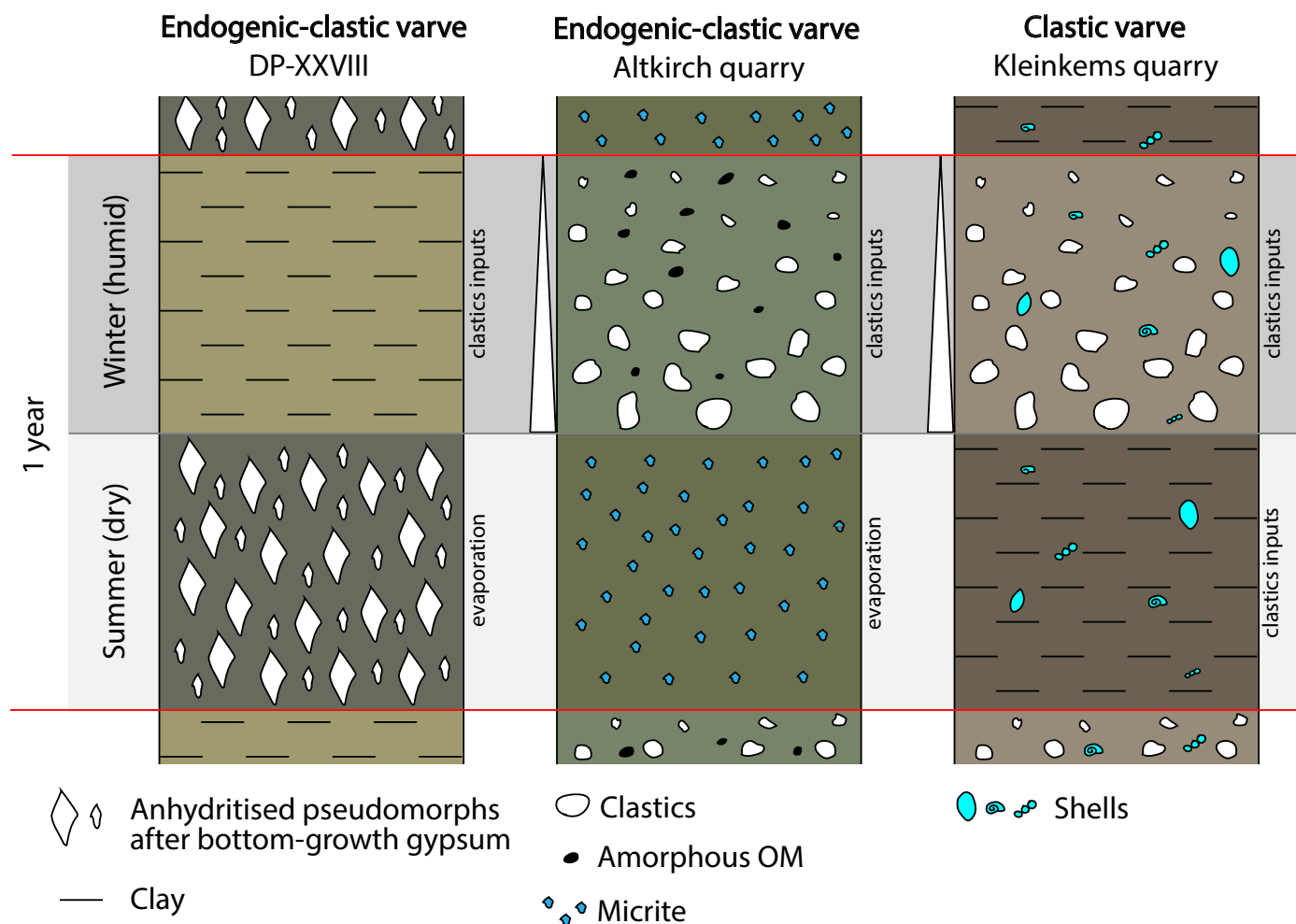


**Figure 9** | Interpretative deposition model for the formation of three types of varves identified for the southern Upper Rhine Graben through the late Priabonian and Rupelian. The main climate variation that causes the seasonality of depositional processes are the changes in precipitation due to dry summers and humid winters.

#### 5.1.2.2. Proximal records (Altkirch and Kleinkems quarries; "Zone Fossilifère")

The samples from the Altkirch (southern river fan delta) and Kleinkems (fan-delta related to the eastern border fault; Düringer, 1988) quarries display couplets of dark- and light-colored laminae. The light-colored laminae contain large amounts of detrital silt-sized grains. We propose that they were delivered by fluvial runoff during the wet season. Grains comprise a diverse mineral assemblage, with calcite and quartz derived from the erosion of the surrounding uplifted Mesozoic (and Paleozoic) rift shoulders. While quartz grains are clearly detrital, calcite crystals could either be autochthonous or allochthonous (e.g., reworked from Jurassic limestones). In the case of the Altkirch Quarry, the presence of organic matter, mostly alongside detrital grains, suggests that it is of detrital origin. Furthermore, terrestrial macrofossils such as plant debris account for a fluvial sediment source in these deposits (Figure 6B; Gaudant & Burkhardt, 1984; Düringer, 1988). The light-colored laminae show fining-up sequences, which suggests that they record a flood (pulse event) during the wet season, rather than a continuous accumulation of sediment through multiple months. The varying thickness of these laminae could reflect year-to-year

climatic variability, with the thicker laminae possibly representing winters with more intense precipitation. However, this could also be explained solely by internal fluvial processes, such as channel migration or sediment availability. The dark-colored laminae are homogenous and made of thin micrite (likely aragonite) crystals. The absence of lithogenic elements (Si, Fe, K) in the dark-colored laminae indicates the absence of detrital material, which suggests that the micrite crystals are endogenic (formed in the water column) rather than detrital. These interpretations are supported by the elemental profiles that clearly distinguish between endogenic carbonated laminae (enriched in Ca with no lithogenic elements) and detrital laminae (enriched in lithogenic elements; Figure 5). Furthermore, these couplets are very similar to the Holocene clastic-calcitic varves of Lake Chatyr Kol, for which the seasonal deposition pattern is supported by radiometric dating, even though they contain less sub-layers (Kalanke et al., 2020). These varves exhibit a detrital layer with a sharp basal boundary (runoff), with chrysophytes and/or diatoms occurring after or within it, overlain by a layer of endogenic (evaporation) and fine-grain detrital calcite, which is topped by an amorphous organic matter sub-layer. Therefore, by comparison with the varves of Lake Chatyr Kol, and according to

petrographical and geochemical evidence presented in this study, we interpret the clastic-endogenic couplets of the Altkirch Quarry as varves.

In the case of the Kleinkems Quarry, the presence of lithogenic elements in the dark-colored laminae suggests a persistent input of detrital material even during the dry season. This observation leads us to the interpretation of both the dark- and light-colored laminae couplets of this quarry as solely clastic varves that show seasonal changes in grain-size. However, it is not impossible that the dark-colored laminae are endogenic (similarly to the clastic-calcitic varves of Lake Chatyr Kol; Kalanke et al., 2020), and that the proximity of the depositional area with the border fault accounts for occasional detrital input.

### 5.1.2.3. Sediment accumulation rates

Considering the ~2 mm varve thickness of the "Sel III" unit (Figure 4), the average SAR is estimated at ~2 m/kyr. This SAR would imply that precession cycles would be ~40 m thick, which is much more than the observed ~12.6 m thick mudstone-evaporite alternations of the "Sel III" unit. It would also imply a SAR higher than any observed rift valley (Schwab, 1976). This estimation however does not account for the potential SAR variations across lithologies, and especially when considering the mudstone intervals, as not all mudstone samples are finely laminated (Figure 3F; see supplementary files). Precise estimates cannot be given here due to the fragmentary nature of the retrieved core samples. Further studies are required to provide more details, such as continuous microfacies descriptions (which would require the collection of new core). However, in the case of the lowermost "Zone Salifère Supérieure", SARs from fine laminations interpreted as varves (Kühn & Roth, 1979) have been used to interpret that the decimeter-thick mudstone-evaporite alternations are as induced by precession in the MAX borehole (Blanc-Valleron et al., 1989; Blanc-Valleron, 1990). We performed the spectral analysis of a part of the "Zone Salifère Supérieure" to provide an independent argument for the interpretation of the meter-thick to decimeter-thick mudstone-evaporite alternations as being astronomically-forced (Figure 8).

## 5.2. Cycle interpretation

The ratios between the ~82.3 m, ~22.4 m, ~9 m, and ~4.5 m sedimentary cycles (DP-212 well, "Sel V") in the depth domain (18.3 : 5 : 2 : 1) (Figure 8) are particularly close to those of the orbital cycles (long eccentricity, short eccentricity, obliquity, and precession) in the time domain (20 : 5 : 2 : 1). The ~82.3 m cycle is therefore interpreted as corresponding to the long eccentricity, the ~22.4 m cycle to short eccentricity, the ~9 m cycle to obliquity, and the ~4.5 m cycle to precession. Furthermore, the ~4.5 m sedimentary cycle has three main peaks that can be correlated to the three main periods of precession. The fact that the ~4.5 m cycle is in phase with the majority of observed mudstone-evaporite alternations suggests that they were

primarily induced by precession through the "Sel V" unit (Figure 8). By comparison, this interpretation confirms the previous investigation of Blanc-Valleron et al. (1989) that suggests that the mudstone-evaporite cycles of the "Sel III" were astronomically-forced.

## 5.3. Facies change across the EOT: a marker of regional climatic change with implications for global climate dynamics

The facies transition from massive mudstones to laminated sediments and varves along the onset of the meter-thick to decimeter-thick mudstone-evaporite alternations is well-documented in the original description of the DP-XXVIII well (MDPA, 1960). Until now, it was neither discussed, nor placed in the perspective of the EOT (Figures 2 and 3). The two main drivers of change in sedimentary facies are climate and tectonics (Carroll & Bohacs, 1999). The climatic evolution of the URG during the Eocene and Oligocene is relatively well-known and reveals a marked increase in the seasonal climatic contrast at the bottom of the "Sel III" unit (Schuler, 1988). Climatic conditions shifted from wet subtropical during the "Zone Salifère Inférieure", with a short or absent dry season, to the drier subtropical/mediterranean-type conditions of the "Zone Salifère Moyenne", with a pronounced dry season lasting around half the year. This shift is penecontemporaneous with the facies transition, and we therefore argue that this change in sedimentary facies reflects the onset of a pronounced seasonal climatic contrast. In addition, the onset of laminated sediments and varves is also synchronous with the onset of repetitive decimeter-thick marl-evaporite alternations. The study of Blanc-Valleron et al. (1989), and the spectral analysis of the DP-212 well presented in this paper, suggest that these alternations are forced by precession in the "Zone Salifère Supérieure" (Figures 2 and 8), and in the "Sel III" as well by comparison.

In paleoenvironmental terms of the classification of lake-basin types (Carroll & Bohacs, 1999; Bohacs et al., 2000), the deposits of the "Zone Salifère Inférieure", "Zone Salifère Moyenne", and "Zone Salifère Supérieure" are characteristic of an underfilled lake. The relative stability of the climate across the deposition of the "Zone Salifère Inférieure" (Schuler, 1988) suggests that these lithological changes were potentially not driven by climatic changes. Starting from the bottom of the "Sel III", the decimeter-thick mudstone-evaporite cycles were most likely induced by lake-level variations related to orbital cycles. While we emphasize that the varves resulted from seasonal precipitation changes, with the clastic laminae being deposited during humid winters and chemical laminae deposited during dry summers (potentially associated to seasonal lake-level fluctuations), it is also possible that seasonal temperature changes influenced the saturation of brines. By comparison, facies changes associated with an increase in seasonal climatic contrast have been documented further west in the Rennes Basin across the EOT (Tramoy et al., 2016; Bauer et al., 2016; Boulila et al., 2021).



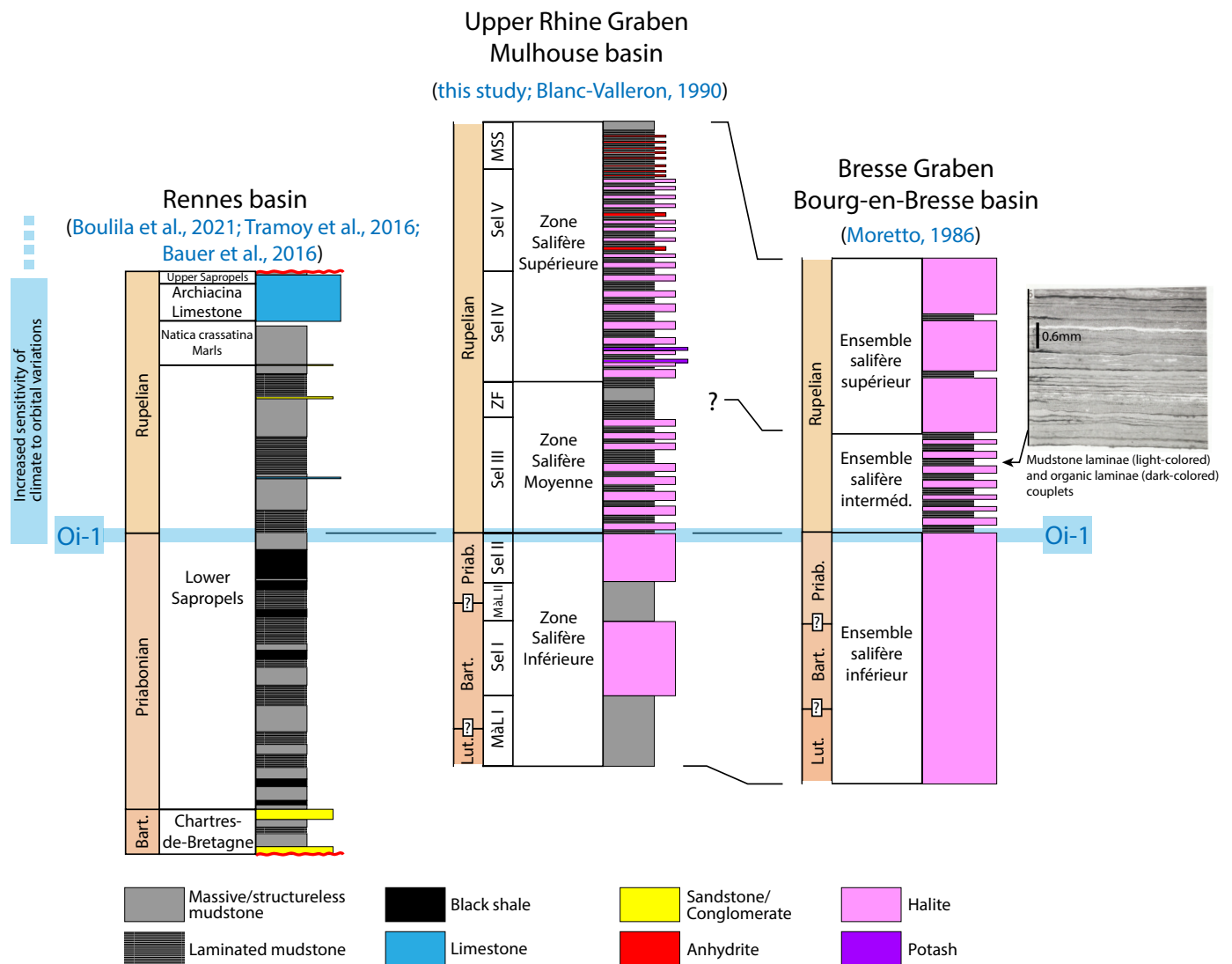


**Figure 10** | Comparison and correlations between the sedimentary records of the Rennes (Bauer et al., 2016; Tramoy et al., 2016; Boulila et al., 2021), Mulhouse (Blanc-Valleron, 1990; this study), and Bourges (Moretto, 1986) basins.

In the Rennes Basin, a sharp contact between massive, clotted greenish clays, and brownish, organic laminated clays is described above the Eocene-Oligocene boundary (Oi-1 event) (Boulila et al., 2021). However, the microfacies of the laminated clays were not analyzed in detail and their depositional processes and potential cyclicity (i.e., as varved deposits) were not assessed. Furthermore, laminated mudstones are also described earlier in the sequence and are attributed to hypoxic lacustrine conditions. Detailed microfacies investigations would be required to assess whether these laminated sediments show significant facies changes before and after the EOT. The detailed cyclostratigraphy of the Rennes Basin indicates strengthening of the eccentricity and the precession band at the EOT (Boulila et al., 2021). There are therefore strong similarities between the Mulhouse Basin and the Rennes Basin, as both basins display pronounced facies changes with the presence of laminated sediments and astronomically-forced sedimentary alternations. Furthermore, the Bourges Basin (Bresse Graben), similar to the Mulhouse Basin, exhibits the onset of decimeter-thick mudstone-evaporite alternations in which mudstones are laminated and display light-colored (carbonated) and

dark-colored (organic) sub-millimeter-thick couplets that resemble varves (Moretto, 1986) (Figure 10). The bottom of the "Ensemble Salifère Intermédiaire" of the Bourges Basin has been correlated to the bottom of the "Sel III" of the Mulhouse Basin (Moretto, 1986; Blanc-Valleron, 1990), and both basins display an increase in seasonal climatic contrast at that time (Schuler, 1988). The combined observations of these three records (which are several hundreds of kilometers apart) provide evidence for an increase in seasonal climatic contrast and in sensitivity of the climate to orbital variations over the continental west European mid-latitudes during the EOT. This hypothesis is consistent with recent studies that suggest an increase in sensitivity of the climate to orbital variations across the EOT (Westerhold et al., 2020; Tardif et al., 2021).

This prominent change in sedimentary regime occurs over a short stratigraphic interval and marks a change-point in the evolution of the behavior of the lacustrine systems that occupied the three basins. All these characteristics match well with the definition of a xenoconformity, which describes a stratigraphic surface (or gradational interval) that records an abrupt change in sedimentary facies across

regional to global scales (Carroll, 2017). The intra-basinal to inter-basinal recognition of such a singular stratigraphic surface or interval is therefore interpreted as diagnostic of major global climate changes, such as that of the Oi-1 event (and EOT) observed in western Eurasia mid-latitude lacustrine records (Boulila et al., 2016; Ao et al., 2020). We thus propose that the increase in seasonal climatic contrast and sensitivity of climate to orbital variations observed in the Mulhouse and Bourg-en-Bresse basins are, similarly, synchronous with the EOT.

Compared to investigations performed at other localities, our findings better assess regional and global coherency (and therefore potential driving mechanisms) of the observed changes. High resolution marine  $\delta^{13}\text{C}$  and  $\delta^{18}\text{O}$  benthic records suggest increased sensitivity of the climate to orbital variations across the EOT, which are linked to the formation of the Antarctic ice sheet and resulting increased oceanic circulation dynamics at seasonal and orbital scales (see Westerhold et al., 2020 and references therein). This provides a simple explanation for the increased seasonal climatic contrast observed in western Europe and is substantiated by further studies. The study of North Atlantic sediment cores revealed the change from diverse mixed broad-leaved to cooler conifer-dominated pollen, indicative of an increase in seasonal climatic contrast across the EOT (Eldrett et al., 2009). Geochemical analyses performed on shells of freshwater gastropods in the Hampshire Basin (United Kingdom) indicate a decrease in growing-season surface temperatures of 4°C across the EOT, indicating that the change in seasonal climatic contrast was likely also expressed by colder winters (Hren et al., 2013). Other studies account for a shift from warm paratropical/temperate to temperate/boreal vegetation in western and central Europe, which is also indicative of an increase in seasonal climatic contrast across the EOT (Mosbrugger et al., 2005; Kvaček et al., 2014; Utescher et al., 2015; Kunzmann et al., 2016). Continental temperature curves derived from central Europe flora have been correlated to global marine oxygen isotopes, suggesting a tight link between continental climate with oceanic changes and Antarctic ice-sheet (Mosbrugger et al., 2005), as well as the interpretation that pCO<sub>2</sub> drawdown and associated temperature drop that may have simply led to dryer and cooler winters, thus enhancing seasonal climatic contrasts (Eldrett et al., 2009). Furthermore, these observations are similar to a distant record in northeastern Tibet, where a transition from sedimentary cycles dominated by eccentricity to sedimentary cycles paced by a combination of eccentricity, obliquity, and precession is observed across the Oi-1 event (Ao et al., 2020). This suggests increased seasonality extended at least over the Eurasian continent across the EOT. However, this trend does not appear to extend globally, as indicated by recent proxy-data reviews across the EOT (Hutchinson et al., 2019) and data-model comparisons (Tardif et al., 2021; Toumoulin et al., 2022), most notably in North America showing only limited variability increases. This implies the EOT affected Eurasia climate patterns differently and led

to the suggested increase in modulations of the westerlies (Toumoulin et al., 2022). Most importantly, teleconnections in circulation changes in the North Atlantic following the formation of the Antarctic ice-sheet has been proposed to relate to the onset and/or strengthening of the AMOC (Goldner et al., 2014). Such a mechanism would affect the seasonal climatic contrast and the sensitivity of local climate to orbital forcing in Eurasian mid-latitude records (Goldner et al., 2014). It should be noted, however, that more recent numerical simulations considering the pCO<sub>2</sub> reduction, the Antarctic ice-sheet development, as well as gateway opening around Antarctica associated with sea-level drop, fail to reproduce strengthening of AMOC-like oceanic dynamics (see Toumoulin et al., 2020 and references therein). Recent studies have also linked the EOT to gateway opening and closing between the Atlantic and the proto-Arctic (Coxall et al., 2018; Straume et al., 2022). These changes may have affected atmospheric and oceanic circulation globally and certainly induced changes in western Europe during the EOT.

Further investigations are required to determine more precisely the links and contributions between global drivers such as pCO<sub>2</sub> drawdown, sea-level drop, and tectonically-forced changes in oceanic circulation (Kennett, 1977; DeConto & Pollard, 2003; Pearson et al., 2009; Abelson & Erez, 2017; Toumoulin et al., 2020; Straume et al., 2022) of European climates across the EOT. This requires the determination of the exact timing of the observed changes in seasonality and astronomically-forced cyclicity through the various phases of the EOT (e.g., Boulila et al., 2021), in combination with numerical model simulations focusing on these particular entities.

## 6. Conclusion

This paper provides insights into the enhancement of seasonal climatic contrast and sensitivity of the local climate to orbital variations across the Eocene-Oligocene Transition in the Upper Rhine Graben. Our new results are based on analyses of sedimentary rock cores and documents from the DP-XXVIII and DP-212 wells, as well as rock samples from the Altkirch and Kleinkems quarries (proximal records; "Zone Fossilifère"). Our investigation provides a new perspective on climate change during the Eocene-Oligocene Transition, the impact upon the lacustrine record of the Upper Rhine Graben, and how this related to global climate dynamics.

1. The presence of varves in the "Sel III" and "Zone Fossilifère" units of the DP-XXVIII well, and in the "Zone Fossilifère" unit of the Altkirch and Kleinkems quarries is proposed based on microfacies analysis, together with a model combining fabric formation and depositional hydrology. We compared the lower Oligocene varves of the Mulhouse Basin to those from the Dead Sea (Ben Dor et al., 2019), and the varves of the Altkirch and Kleinkems quarries ("Zone

Fossilifère”) to those from the Chatyr Kol Lake (Kalanke et al., 2020).

- In the DP-XXVIII well, a strong facies transition from massive mudstones to laminated and varved mudstones is documented from the base of the “Sel III” unit. This change in sedimentary pattern coincides with the onset of decimeter-thick mudstone-evaporite cycles, which we demonstrate are induced by orbital variations. Palynological studies have shown a penecontemporaneous change in climatic conditions towards a mediterranean climate with enhanced seasonal climatic contrast (Schuler, 1988). We thus propose that the appearance of the laminated and varved mudstones records a stronger contrast in the sedimentation processes that resulted from the climate change towards a stronger seasonal climatic contrast. We also suggest that the onset of the decimeter-thick mudstone-evaporite cycles is related to an increase of the sensitivity of the climate to orbital variations across the EOT.
- We outlined similarities between our observations in the Upper Rhine Graben and changes in sedimentary facies documented in the Rennes Basin during the Eocene-Oligocene Transition (Boulila et al., 2021), and in the Bourg-en-Bresse Basin (Moretto, 1986). As such, we suggest that this spatially-transgressive facies transition could be the marker of the Eocene-Oligocene Transition in European mid-latitude lacustrine records. By comparison with similar observations performed in northeastern Tibet, this change could be a marker of the Oi-1 event (Ao et al., 2020). The characterization of such changes in sedimentary facies could help understand climate change during the Eocene-Oligocene Transition and aid the establishment of chronological frameworks. In addition, we suggest that the abruptness of this transition in the Mulhouse, Bourg-en-Bresse, and Rennes basins could reflect a changepoint that had a major impact on regional climate, possibly through a pCO<sub>2</sub> drop and/or oceanic circulation changes, such as the onset of a proto-AMOC in relation with the formation of the Antarctic icesheet. We also show that these observations are coherent with other coeval paleoclimatic records in Europe.

## Acknowledgments

We are grateful to the Musée d’Histoire Naturelle et d’Ethnographie de Colmar (Martial BOUTANTIN, Cl  tre PR  TRE, Manuelle VIGNES) for providing access to the core samples from the DP-XXVIII well, and to the Kalivie Museum (Chantal VIS, Lo  c DEMESY) for providing access to the original written descriptions by MDPa of the DP-XXVIII well. We thank Magalie LINDENMAYER from the Holcim Quarry in Altkirch for allowing us to retrieve samples from the quarry. We thank Kirsten GRIMM and Matthias GRIMM for insightful discussions on the

biostratigraphy of the Upper Rhine Graben. The PhD of ES is funded by MESRI and R  gion Grand-Est. Field work and analysis were funded by a research grant from CNRS/INSU (TelluS/SysTer program) attributed to MS. Additional support was provided by the “Geological Systems” research team at ITES. We are grateful to Ola KWIECIEN and Nicolas WALDMANN for reviewing the manuscript and providing insightful comments.

## Authors contribution

ES wrote the paper, performed sedimentary facies analysis (with LGC, FG, HV and MS). All authors contributed to interpretation and discussion of the results. ES and MS worked on the illustrations and collected field samples. ES and LGC worked on the logging and description of the DP-XXVIII well. MU performed the  $\mu$ -XRF analyses and helped the interpretation. ES and CB worked on the  $\mu$ -XRF results and on the interpretation of varves and laminated sediments. MS and HV designed the overall research project dedicated to the EOT in the URG, and group discussions allowed to sharply define the topic of this paper. GDN provided insights and discussions in regard to the EOT. MM provided insights and discussions in regard to cyclostratigraphy and paleoclimates. LGC provided insights and discussions on evaporites, cores, and on the URG. FG provided insights and discussions on the URG and cores. CB, LGC, HV and MS provided expertise on laminated sediments and varves.

## Data availability

All the data presented in this publication can be downloaded from the website of Sedimentologica.

## Conflict of interest

The authors declare no conflict of interest.

## References

- Abelson, M., & Erez, J. (2017). The onset of modernlike Atlantic meridional overturning circulation at the Eocene-Oligocene transition: Evidence, causes, and possible implications for global cooling. *Geochemistry, Geophysics, Geosystems*, 18(6), 2177-2199. <https://doi.org/10.1002/2017GC006826>
- Aichholzer, C. (2019). Le log complet de la stratigraphie de la zone rh  nane ainsi que les modalit  s stratigraphiques, s  dimentaires et structurales de la transition socle-couverture: application    la g  othermie profonde (Doctoral dissertation, Universit   de Strasbourg).
- Ao, H., Dupont-Nivet, G., Rohling, E. J., Zhang, P., Ladant, J. B., Roberts, A. P., Licht, A., Liu, Q., Liu, Z., Dekkers, M. J., Coxall, H. K., Jin, Z., Huang, C., Xiao, G., Poulsen, C. J., Barbolini, N., Meijer, N., Sun, Q., Qiang, X., Yao, J., & An, Z. (2020). Orbital climate variability on the northeastern Tibetan Plateau across the Eocene–Oligocene transition. *Nature Communications*, 11(1), 5249. <https://doi.org/10.1038/s41467-020-18824-8>
- Bauer, H., Bessin, P., Saint-Marc, P., Ch  teau-neuf, J. J., Bourdillon, C., Wyns, R., & Guillocheau, F. (2016). The Cenozoic history of the Armorican Massif: New insights from the deep CDB1 borehole

- (Rennes Basin, France). *Comptes Rendus Geoscience*, 348(5), 387-397. <https://doi.org/10.1016/j.crte.2016.02.002>
- Ben Dor, Y. B., Neugebauer, I., Enzel, Y., Schwab, M. J., Tjallingii, R., Erel, Y., & Brauer, A. (2019). Varves of the Dead Sea sedimentary record. *Quaternary Science Reviews*, 215, 173-184. <https://doi.org/10.1016/j.quascirev.2019.04.011>
- Berger, J. P., Reichenbacher, B., Becker, D., Grimm, M., Grimm, K., Picot, L., Storni, A., Pirkenseer, C., & Schaefer, A. (2005). Eocene-Pliocene time scale and stratigraphy of the Upper Rhine Graben (URG) and the Swiss Molasse Basin (SMB). *International Journal of Earth Sciences*, 94, 711-731. <https://doi.org/10.1007/s00531-005-0479-y>
- Blanc-Valleron, M. M. (1990). Les formations paléogènes évaporitiques du bassin potassique de Mulhouse et des bassins plus septentrionaux d'Alsace. Documents BRGM, Vol. 204, 350 p.
- Blanc-Valleron, M. M., Foucault, A., & Gannat, E. (1989). Le contrôle climatique, orbital, et solaire de la sédimentation évaporitique : exemple de la base du Salifère supérieur (Oligocène inférieur) du bassin de Mulhouse (Sud du fossé rhénan, France). *Comptes rendus de l'Académie des sciences. Série 2, Mécanique, Physique, Chimie, Sciences de l'univers, Sciences de la Terre*, 308(4), 435-441.
- Boës, X., Rydberg, J., Martinez-Cortizas, A., Bindler, R., & Renberg, I. (2011). Evaluation of conservative lithogenic elements (Ti, Zr, Al, and Rb) to study anthropogenic element enrichments in lake sediments. *Journal of Paleolimnology*, 46, 75-87. <https://doi.org/10.1007/s10933-011-9515-z>
- Bohacs, K. M., Carroll, A. R., Neal, J. E., & Mankiewicz, P. J. (2000). Lake-Basin Type, Source Potential, and Hydrocarbon Character: an Integrated Sequence-Stratigraphic-Geochemical Framework, in E. H. Gierlowski-Kordesch and K. R. Kelts, eds., *Lake basins through space and time: AAPG Studies in Geology*, 46, 3-34. <https://doi.org/10.1306/St46706C1>
- Bohaty, S. M., Zachos, J. C., & Delaney, M. L. (2012). Foraminiferal Mg/Ca evidence for Southern Ocean cooling across the Eocene-Oligocene transition. *Earth and Planetary Science Letters*, 317, 251-261. <https://doi.org/10.1016/j.epsl.2011.11.037>
- Boulila, S., Dupont-Nivet, G., Galbrun, B., Bauer, H., & Châteauneuf, J. J. (2021). Age and driving mechanisms of the Eocene-Oligocene transition from astronomical tuning of a lacustrine record (Rennes Basin, France). *Climate of the Past*, 17(6), 2343-2360. <https://doi.org/10.5194/cp-17-2343-2021>
- Brauer, A., Dulski, P., Mangili, C., Mingram, J., & Liu, J. (2009). The potential of varves in high-resolution paleolimnological studies. *PAGES news*, 17(3), 96-98. <https://doi.org/10.22498/pages.17.3.96>
- Carroll, A.R., 2017, Xenconformities and the stratigraphic record of paleoenvironmental change: *Geology*, v. 45, p. 639-642. <https://doi.org/10.1130/G38952.1>
- Carroll, A. R., & Bohacs, K. M. (1999). Stratigraphic classification of ancient lakes: Balancing tectonic and climatic controls. *Geology*, 27(2), 99-102. [https://doi.org/10.1130/0091-7613\(1999\)027<0099:SCOALB>2.3.CO;2](https://doi.org/10.1130/0091-7613(1999)027<0099:SCOALB>2.3.CO;2)
- Châteauneuf, J. J., & Ménéillet, F. (2014). A Bartonian microflora record from the Upper Rhine Graben: the Mietesheim formation (Alsace, France). *Géologie de la France*, (1), 3-20.
- Courtot, C., Gannat, E., & Wendling, E. (1972). Le bassin potassique de Mulhouse et ses environs. Étude du Tertiaire. *Sciences Géologiques, bulletins et mémoires*, 25(2), 69-91.
- Coxall, H. K., Huck, C. E., Huber, M., Lear, C. H., Legarda-Lisarri, A., O'regan, M., Sliwinska K. K., van de Fliedrt, T., de Boer, A. M., Zachos, J. C., & Backman, J. (2018). Export of nutrient rich Northern Component Water preceded early Oligocene Antarctic glaciation. *Nature Geoscience*, 11(3), 190-196. <https://doi.org/10.1038/s41561-018-0069-9>
- Coxall, H. K., Wilson, P. A., Pälike, H., Lear, C. H., & Backman, J. (2005). Rapid stepwise onset of Antarctic glaciation and deeper calcite compensation in the Pacific Ocean. *Nature*, 433(7021), 53-57. <https://doi.org/10.1038/nature03135>
- Davies, S. J., Lamb, H. F., & Roberts, S. J. (2015). Micro-XRF Studies of Sediment Cores: Applications of a non-destructive tool for the environmental sciences. *Developments in Paleoenvironmental Research*, 17, 189-226. [https://doi.org/10.1007/978-94-017-9849-5\\_7](https://doi.org/10.1007/978-94-017-9849-5_7)
- DeConto, R. M., & Pollard, D. (2003). Rapid Cenozoic glaciation of Antarctica induced by declining atmospheric CO<sub>2</sub>. *Nature*, 421(6920), 245-249. <https://doi.org/10.1038/nature01290>
- Dèzes, P., Schmid, S. M., & Ziegler, P. A. (2004). Evolution of the European Cenozoic Rift System: interaction of the Alpine and Pyrenean orogens with their foreland lithosphere. *Tectonophysics*, 389(1-2), 1-33. <https://doi.org/10.1016/j.tecto.2004.06.011>
- Dräger, N., Theuerkauf, M., Szeroczyńska, K., Wulf, S., Tjallingii, R., Plessen, B., Kienel, U., & Brauer, A. (2017). Varve microfacies and varve preservation record of climate change and human impact for the last 6000 years at Lake Tiefer See (NE Germany). *The Holocene*, 27(3), 450-464. <https://doi.org/10.1177/0959683616660173>
- Dupont-Nivet, G., Krijgsman, W., Langereis, C. G., Abels, H. A., Dai, S., & Fang, X. (2007). Tibetan plateau aridification linked to global cooling at the Eocene-Oligocene transition. *Nature*, 445(7128), 635-638. <https://doi.org/10.1038/nature05516>
- Düringer, P. (1988). Les conglomérats des bordures du rift cénozoïque rhénan : dynamique sédimentaire et contrôle climatique. Thèse d'État, Université de Strasbourg, 287p.
- Edel, J. B., Schulmann, K., & Rotstein, Y. (2007). The Variscan tectonic inheritance of the Upper Rhine Graben: evidence of reactivations in the Lias, Late Eocene-Oligocene up to the recent. *International Journal of Earth Sciences*, 96(2), 305-325. <https://doi.org/10.1007/s00531-006-0092-8>
- Eldrett, J. S., Greenwood, D. R., Harding, I. C., & Huber, M. (2009). Increased seasonality through the Eocene to Oligocene transition in northern high latitudes. *Nature*, 459(7249), 969-973. <https://doi.org/10.1038/nature08069>
- Förster B. (1911). Ergebnisse der Untersuchung von Bohrproben aus den seit 1904 im Gange befindlichen, zur Aufsuchung von Steinsaltz und Kalisaltzen ausgeführten Tiefbohrungen im Tertiär des Oberelsass. *Mitt. Geol. Landesanst. Els.-Lothr.*, 7(4), 349-524.
- Gaudant, J., & Burkhardt, T. (1984). Sur la découverte de poissons fossiles dans les marnes grises rayées de la zone fossilifère (Oligocène basal) d'Altkirch (Haut-Rhin). *Sciences Géologiques, bulletins et mémoires*, 37(2), 153-171.
- Goldner, A., Herold, N., & Huber, M. (2014). Antarctic glaciation caused ocean circulation changes at the Eocene-Oligocene transition. *Nature*, 511(7511), 574-577. <https://doi.org/10.1038/nature13597>
- Grimm, M. C., Wielandt-Schuster, U., Hottenrott, M., Radtke, G., Berger, J. P., Ellwanger, D., Harms, F. J., Hoselmann, C. P., & Weidenfeller, M. (2011). Oberrheingraben (Tertiär des Oberrheingrabens). *Schriftenreihe der Deutschen Gesellschaft für Geowissenschaften*, 57-132. <https://doi.org/10.1127/sdgg/75/2011/57>

- Hooker, J. J., Collinson, M. E., & Sille, N. P. (2004). Eocene–Oligocene mammalian faunal turnover in the Hampshire Basin, UK: calibration to the global time scale and the major cooling event. *Journal of the Geological Society*, 161(2), 161–172. <https://doi.org/10.1144/0016-764903-091>
- Hren, M. T., Sheldon, N. D., Grimes, S. T., Collinson, M. E., Hooker, J. J., Bugler, M., & Lohmann, K. C. (2013). Terrestrial cooling in Northern Europe during the Eocene–Oligocene transition. *Proceedings of the National Academy of Sciences*, 110(19), 7562–7567. <https://doi.org/10.1073/pnas.1210930110>
- Hutchinson, D. K., Coxall, H. K., Lunt, D. J., Steinthorsdottir, M., De Boer, A. M., Baatsen, M., von der Heydy, A., Huber, M., Kennedy-Asser, A. T., Kunzmann, L., Ladant, J. B., Lear, C. H., Moraweck, K., Pearson, P. N., Piga, E., Pound, M. J., Salzmann, U., Scher, H. D., Sijp, W. P., Śliwińska, K.K., Wilson, P. A., & Zhang, Z. (2021). The Eocene–Oligocene transition: a review of marine and terrestrial proxy data, models and model–data comparisons. *Climate of the Past*, 17(1), 269–315. <https://doi.org/10.5194/cp-17-269-2021>
- Hutchinson, D. K., Coxall, H. K., O'Regan, M., Nilsson, J., Caballero, R., & de Boer, A. M. (2019). Arctic closure as a trigger for Atlantic overturning at the Eocene–Oligocene Transition. *Nature Communications*, 10(1), 3797. <https://doi.org/10.1038/s41467-019-11828-z>
- Ivany, L. C., Patterson, W. P., & Lohmann, K. C. (2000). Cooler winters as a possible cause of mass extinctions at the Eocene/Oligocene boundary. *Nature*, 407(6806), 887–890. <https://doi.org/10.1038/35038044>
- Kalanke, J., Mingram, J., Lauterbach, S., Usubaliev, R., Tjallingii, R., & Brauer, A. (2020). Seasonal deposition processes and chronology of a varved Holocene lake sediment record from Chatyr Kol lake (Kyrgyz Republic). *Geochronology*, 2(1), 133–154. <https://doi.org/10.5194/gchron-2-133-2020>
- Katz, M. E., Miller, K. G., Wright, J. D., Wade, B. S., Browning, J. V., Cramer, B. S., & Rosenthal, Y. (2008). Stepwise transition from the Eocene greenhouse to the Oligocene icehouse. *Nature geoscience*, 1(5), 329–334. <https://doi.org/10.1038/ngeo179>
- Kennedy, A. T., Farnsworth, A., Lunt, D. J., Lear, C. H., & Markwick, P. J. (2015). Atmospheric and oceanic impacts of Antarctic glaciation across the Eocene–Oligocene transition. *Philosophical Transactions of the Royal Society A: Mathematical, Physical and Engineering Sciences*, 373(2054), 20140419. <https://doi.org/10.1098/rsta.2014.0419>
- Kennett, J. P. (1977). Cenozoic evolution of Antarctic glaciation, the circum-Antarctic Ocean, and their impact on global paleoceanography. *Journal of geophysical research*, 82(27), 3843–3860. <https://doi.org/10.1029/JC082i027p03843>
- Kohn, M. J., Strömberg, C. A., Madden, R. H., Dunn, R. E., Evans, S., Palacios, A., & Carlini, A. A. (2015). Quasi-static Eocene–Oligocene climate in Patagonia promotes slow faunal evolution and mid-Cenozoic global cooling. *Palaeogeography, Palaeoclimatology, Palaeoecology*, 435, 24–37. <https://doi.org/10.1016/j.palaeo.2015.05.028>
- Kühn, R., & Roth, H. (1979). Beiträge zur Kenntnis der Salzlagerstätte am Oberrhein. *Z. Geol. Wiss.*, 7, 953–966.
- Kunzmann, L., Kvaček, Z., Teodoridis, V., Müller, C., & Moraweck, K. (2016). Vegetation dynamics of riparian forest in central Europe during the late Eocene. *Palaeontographica Abteilung B*, 69–89. <https://doi.org/10.1127/palb/295/2016/69>
- Kvaček, Z., Teodoridis, V., Mach, K., Příkryl, T., & Dvořák, Z. (2014). Tracing the Eocene–Oligocene transition: a case study from North Bohemia. *Bulletin of Geosciences*, 89(1). <https://doi.org/10.3140/bull.geosci.1411>
- Kwiecien, O., Braun, T., Brunello, C. F., Faulkner, P., Hausmann, N., Helle, G., Hoggarth, J. A., Ionita, M., Jazwa, C. S., Kelmelis, S., Marwan, N., Nava-Fernandez, C., Nehme, C., Opel, T., Oster, J. L., Perşoiu, A., Petrie, C., Pruffer, K., Saarni, S. M., Wolf, A., & Breitenbach, S. F. (2022). What we talk about when we talk about seasonality—A transdisciplinary review. *Earth-Science Reviews*, 225, 103843. <https://doi.org/10.1016/j.earscirev.2021.103843>
- Ladant, J. B., Donnadiou, Y., Lefebvre, V., & Dumas, C. (2014). The respective role of atmospheric carbon dioxide and orbital parameters on ice sheet evolution at the Eocene–Oligocene transition. *Paleoceanography*, 29(8), 810–823. <https://doi.org/10.1002/2013PA002593>
- Lear, C. H., Bailey, T. R., Pearson, P. N., Coxall, H. K., & Rosenthal, Y. (2008). Cooling and ice growth across the Eocene–Oligocene transition. *Geology*, 36(3), 251–254. <https://doi.org/10.1130/G24584A.1>
- Li, M., Hinnov, L., & Kump, L. (2019). Acycle: Time-series analysis software for paleoclimate research and education. *Computers & Geosciences*, 127, 12–22. <https://doi.org/10.1016/j.cageo.2019.02.011>
- Liu, Z., Pagani, M., Zinniker, D., DeConto, R., Huber, M., Brinkhuis, H., Shah, S. R., Leckie, R. M., & Pearson, A. (2009). Global cooling during the Eocene–Oligocene climate transition. *Science*, 323(5918), 1187–1190. <https://doi.org/10.1126/science.1166368>
- Maïkovsky, V. (1941). Contribution à l'étude paléontologique et stratigraphique du bassin potassique d'Alsace. *Mémoires du Service de la Carte géologique d'Alsace et de Lorraine*, Vol. 6, 192 p.
- Mann, M. E., & Lees, J. M. (1996). Robust estimation of background noise and signal detection in climatic time series. *Climatic change*, 33(3), 409–445. <https://doi.org/10.1007/BF00142586>
- MDPA (1960). *Catalogue des puits et sondages du bassin de Mulhouse*, Vol. XIV, 3–119. Miller, K. G., Browning, J. V., Schmelz, W. J., Kopp, R. E., Mountain, G. S., & Wright, J. D. (2020). Cenozoic sea-level and cryospheric evolution from deep-sea geochemical and continental margin records. *Science advances*, 6(20), <https://doi.org/10.1126/sciadv.aaz1346>
- Miller, K. G., Browning, J. V., Schmelz, W. J., Kopp, R. E., Mountain, G. S., & Wright, J. D. (2020). Cenozoic sea-level and cryospheric evolution from deep-sea geochemical and continental margin records. *Science Advances*, 6(20), eaaz1346. <https://doi.org/10.1126/sciadv.aaz1346>
- Miller, K. G., Wright, J. D., & Fairbanks, R. G. (1991). Unlocking the ice house: Oligocene–Miocene oxygen isotopes, eustasy, and margin erosion. *Journal of Geophysical Research: Solid Earth*, 96(B4), 6829–6848. <https://doi.org/10.1029/90JB02015>
- Mingram, J. (1998). Laminated Eocene maar-lake sediments from Eckfeld (Eifel region, Germany) and their short-term periodicities. *Palaeogeography, Palaeoclimatology, Palaeoecology*, 140(1–4), 289–305. [https://doi.org/10.1016/S0031-0182\(98\)00021-2](https://doi.org/10.1016/S0031-0182(98)00021-2)
- Moretto, R. (1986). Étude sédimentologique et géochimique des dépôts de la série salifère paléogène du bassin de Bourg-en-Bresse (France) (Doctoral dissertation, Université de Lorraine).
- Mosbrugger, V., Utescher, T., & Dilcher, D. L. (2005). Cenozoic continental climatic evolution of Central Europe. *Proceedings of the National Academy of Sciences*, 102(42), 14964–14969. <https://doi.org/10.1073/pnas.0505267102>
- Ojala, A. E., Francus, P., Zolitschka, B., Besonen, M., & Lamoureux, S. F. (2012). Characteristics of sedimentary varve

- chronologies—a review. *Quaternary Science Reviews*, 43, 45-60. <https://doi.org/10.1016/j.quascirev.2012.04.006>
- Page, M., Licht, A., Dupont-Nivet, G., Meijer, N., Barbolini, N., Hoorn, C., Schauer, A., Huntington, K., Bajnai, D., Fiebig, J., Mulch, A., & Guo, Z. (2019). Synchronous cooling and decline in monsoonal rainfall in northeastern Tibet during the fall into the Oligocene icehouse. *Geology*, 47(3), 203-206. <https://doi.org/10.1130/G45480.1>
- Pearson, P. N., Foster, G. L., & Wade, B. S. (2009). Atmospheric carbon dioxide through the Eocene–Oligocene climate transition. *Nature*, 461(7267), 1110-1113. <https://doi.org/10.1038/nature08447>
- Pearson, P. N., McMillan, I. K., Wade, B. S., Jones, T. D., Coxall, H. K., Bown, P. R., & Lear, C. H. (2008). Extinction and environmental change across the Eocene-Oligocene boundary in Tanzania. *Geology*, 36(2), 179-182. <https://doi.org/10.1130/G24308A.1>
- Pirkenseer, C., Spezzaferri, S., & Berger, J. P. (2010). Palaeoecology and biostratigraphy of the Paleogene Foraminifera from the southern Upper Rhine Graben and the influence of reworked planktonic Foraminifera. *Palaeontographica, Palaeontographica, Abt. A: Palaeozoology–Stratigraphy*, 293, 1-93.
- Priestley, M. B. (1981). *Spectral analysis and time series: probability and mathematical statistics*. Academic Press, London, 1-890.
- Roussé, S. (2006). *Architecture et dynamique des séries marines et continentales de l'oligocène moyen et supérieur du sud du fossé rhénan : Evolution des milieux de dépôt en contexte de rift en marge de l'avant-pays alpin* (Doctoral dissertation, Université de Strasbourg).
- Sarkar, S., Basak, C., Frank, M., Berndt, C., Huuse, M., Badhani, S., & Bialas, J. (2019). Late Eocene onset of the proto-Antarctic circumpolar current. *Scientific reports*, 9(1), 10125. <https://doi.org/10.1038/s41598-019-46253-1>
- Schuler, M. (1988). *Environnements et paléoclimats paléogènes. Palynologie et biostratigraphie de l'Éocène et de l'Oligocène inférieur dans les fossés rhénan, rhodanien et de Hesse*. Documents BRGM, Vol. 190, 503 p.
- Schumacher, M. E. (2002). Upper Rhine Graben: role of preexisting structures during rift evolution. *Tectonics*, 21(1), 6-1. <https://doi.org/10.1029/2001TC900022>
- Schwab, F. L. (1976). Modern and ancient sedimentary basins: comparative accumulation rates. *Geology*, 4(12), 723-727. [https://doi.org/10.1130/0091-7613\(1976\)4<723:MAASBC>2.0.CO;2](https://doi.org/10.1130/0091-7613(1976)4<723:MAASBC>2.0.CO;2)
- Simon, E., Gindre-Chanu, L., Nutz, A., Boesch, Q., Dupont-Nivet, G., Vogel, H., Schuster, M. (2021). Regard sur un changement climatique majeur : la transition Éocène-Oligocène dans le Fossé Rhénan. *Géologues*, 210, 26-34.
- Sirota, I., Enzel, Y., & Lensky, N. G. (2017). Temperature seasonality control on modern halite layers in the Dead Sea: In situ observations. *Bulletin*, 129(9-10), 1181-1194. <https://doi.org/10.1130/B31661.1>
- Sittler, C. (1965). *Le Paléogène des fossés rhénan et rhodanien. Etudes sédimentologiques et paléoclimatiques*. Mém. Serv. Carte Géol. Alsace Lorrain, 24, 392 p.
- Straume, E. O., Nummelin, A., Gaina, C., & Nisancioglu, K. H. (2022). Climate transition at the Eocene–Oligocene influenced by bathymetric changes to the Atlantic–Arctic oceanic gateways. *Proceedings of the National Academy of Sciences*, 119(17). <https://doi.org/10.1073/pnas.2115346119>
- Sturm, M. (1979). Origin and composition of clastic varves. In *Moraines and varves; origin, genesis, classification, Proceedings of an INQUA symposium on genesis and lithology of Quaternary deposits*, 281-285.
- Taner, M. T. (2000). *Attributes Revisited*, Technical Publication. Rock Solid Images, Inc., Houston, Texas.
- Tanner, L. H. (2010). Continental carbonates as indicators of paleoclimate. *Developments in Sedimentology*, 62, 179-214. [https://doi.org/10.1016/S0070-4571\(09\)06204-9](https://doi.org/10.1016/S0070-4571(09)06204-9)
- Tardif, D., Toumoulin, A., Fluteau, F., Donnadiou, Y., Le Hir, G., Barbolini, N., Licht, A., Ladant, J. B., Sepulchre, P., Viovy, N., Hoorn, C., & Dupont-Nivet, G. (2021). Orbital variations as a major driver of climate and biome distribution during the greenhouse to icehouse transition. *Science Advances*, 7(43). <https://doi.org/10.1126/sciadv.abh2819>
- Thomson, D. J. (1982). Spectrum estimation and harmonic analysis. *Proceedings of the IEEE*, 70(9), 1055-1096. <https://doi.org/10.1109/PROC.1982.12433>
- Toumoulin, A., Donnadiou, Y., Ladant, J. B., Batenburg, S. J., Poblete, F., & Dupont-Nivet, G. (2020). Quantifying the Effect of the Drake Passage Opening on the Eocene Ocean. *Paleoceanography and Paleoclimatology*, 35(8), e2020PA003889. <https://doi.org/10.1029/2020PA003889>
- Toumoulin, A., Tardif, D., Donnadiou, Y., Licht, A., Ladant, J. B., Kunzmann, L., & Dupont-Nivet, G. (2022). Evolution of continental temperature seasonality from the Eocene greenhouse to the Oligocene icehouse—a model–data comparison. *Climate of the Past*, 18(2), 341-362. <https://doi.org/10.5194/cp-18-341-2022>
- Tramoy, R., Salpin, M., Schnyder, J., Person, A., Sebilo, M., Yans, J., Vaury, V., Fozzani, J., & Bauer, H. (2016). Stepwise palaeoclimate change across the Eocene–Oligocene transition recorded in continental NW Europe by mineralogical assemblages and  $\delta^{15}\text{N}_{\text{org}}$  (Rennes Basin, France). *Terra Nova*, 28(3), 212-220. <https://doi.org/10.1111/ter.12212>
- Utescher, T., Bondarenko, O. V., & Mosbrugger, V. (2015). The Cenozoic Cooling–continental signals from the Atlantic and Pacific side of Eurasia. *Earth and Planetary Science Letters*, 415, 121-133. <https://doi.org/10.1016/j.epsl.2015.01.019>
- Warren, J. K. (2016). *Evaporites: A geological compendium*. Springer. <https://doi.org/10.1007/978-3-319-13512-0>
- Weedon, G. P. (2003). *Time Series Analysis and Cyclostratigraphy: Examining Stratigraphic Records of Environmental Cycles*. Cambridge University Press. <https://doi.org/10.1017/CBO9780511535482>
- Weltje, G. J., Bloemsmas, M. R., Tjallingii, R., Heslop, D., Röhl, U., & Croudace, I. W. (2015). Prediction of geochemical composition from XRF core scanner data: a new multivariate approach including automatic selection of calibration samples and quantification of uncertainties. *Micro-XRF Studies of Sediment Cores: Applications of a non-destructive tool for the environmental sciences*, 507-534. [https://doi.org/10.1007/978-94-017-9849-5\\_21](https://doi.org/10.1007/978-94-017-9849-5_21)
- Westerhold, T., Marwan, N., Drury, A. J., Liebrand, D., Agnini, C., Anagnostou, E., Barnet, J. S. K., Bohaty, S. M., De Vleeschouwer, D., Florindo, F., Frederichs, T., Hodell, D. A., Holbourn, A. E., Kroon, D., Laurentino, V., Littler, K., Lourens, L. J., Lyle, M., Pälike, H., Röhl, U., Tian, J., Wilkens, R. H., Wilson, P. A., & Zachos, J. C. (2020). An astronomically dated record of Earth's climate and its predictability over the last 66 million years. *Science*, 369(6509), 1383-1387. <https://doi.org/10.1126/science.aba6853>

- Wilson, M. V., & Bogen, A. (1994). Tests of the annual hypothesis and temporal calibration of a 6375-varve fish-bearing interval, Eocene horsefly beds, British Columbia, Canada. *Historical Biology*, 7(4), 325-339. <https://doi.org/10.1080/10292389409380463>
- Zachos, J., Pagani, M., Sloan, L., Thomas, E., & Billups, K. (2001). Trends, rhythms, and aberrations in global climate 65 Ma to present. *science*, 292(5517), 686-693. <https://doi.org/10.1126/science.1059412>
- Zanazzi, A., Judd, E., Fletcher, A., Bryant, H., & Kohn, M. J. (2015). Eocene–Oligocene latitudinal climate gradients in North America inferred from stable isotope ratios in perissodactyl tooth enamel. *Palaeogeography, Palaeoclimatology, Palaeoecology*, 417, 561-568. <https://doi.org/10.1016/j.palaeo.2014.10.024>
- Zolitschka, B., Francus, P., Ojala, A. E., & Schimmelmann, A. (2015). Varves in lake sediments—a review. *Quaternary Science Reviews*, 117, 1-41. <https://doi.org/10.1016/j.quascirev.2015.03.019>

How to cite: Simon, E., Gindre-Chanu, L., Blanchet, C., Dupont-Nivet, G., Martinez, M., Guillocheau, F., Ulrich, M., Nutz, A., Vogel, H., & Schuster, M. (2024). Lacustrine rhythmites from the Mulhouse Basin (Upper Rhine Graben, France): a sedimentary record of increased seasonal climatic contrast and sensitivity of the climate to orbital variations through the Eocene-Oligocene Transition. *Sedimentologica*, 2(1), 1-22. <https://doi.org/10.57035/journals/sdk.2024.e21.1222>

